

# Black hole radiation in Bose-Einstein condensates

Jean Macher\* and Renaud Parentani†

*Laboratoire de Physique Théorique, CNRS UMR 8627,  
Bât. 210, Université Paris-Sud 11, 91405 Orsay Cedex, France*

(Dated: February 16, 2022)

## Abstract

We study the phonon fluxes emitted when the condensate velocity crosses the speed of sound, i.e., in backgrounds which are analogue to that of a black hole. We focus on elongated one dimensional condensates, and on stationary flows. Our theoretical analysis and numerical results are based on the Bogoliubov-de Gennes equation without any further approximation. The spectral properties of the fluxes and of the long distance density-density correlations are obtained, with and without an initial temperature. In realistic conditions, we show that the condensate temperature dominates the fluxes, and thus hides the presence of the spontaneous emission (the Hawking effect). We also explain why the temperature amplifies the long distance correlations which are intrinsic to this effect. This confirms that the correlations pattern offers a neat signature of the Hawking effect. Optimal conditions to observe the pattern are discussed. Applications to flows associated with white holes are briefly considered.

PACS numbers: 03.75.Kk, 04.62.+v, 04.70.Dy

---

\*Electronic address: jean.macher@th.u-psud.fr

†Electronic address: renaud.parentani@th.u-psud.fr

## I. INTRODUCTION

The analogy between sound propagation in nonhomogeneous media and light propagation in curved space-times has opened the possibility to detect the analogue of black hole radiation in the lab [1]. Indeed, when sound waves propagate in a flowing medium whose velocity crosses at some point the speed of sound, they experience the analogue of an event horizon. If the phonon state is stationary and regular across this sonic horizon, one expects to obtain a thermal flux of phonons with a temperature  $k_B T = \hbar \kappa / 2\pi$ , where  $\kappa$  is the gradient of the flow velocity evaluated at the sonic horizon. Since the analogy perfectly works when neglecting the phonon dispersion, the above result should be valid at least when  $\kappa$  is much smaller than the critical wave-vector characterizing the dispersion [2, 3, 4, 5].

Following the original work of Unruh, various setups were proposed, see [6] for a review. In Refs. [7, 8] the particular case of sound waves in dilute Bose-Einstein condensates (BEC) was considered. These condensates have nice properties both from an experimental and a theoretical point of view. From the first, progress in the manipulation and control of their physical properties is rapid, and from the second, the wave equations for the condensate and for the phonons are well understood, as well as the validity of the approximations they involve [9].

In the present work, using analytical and numerical techniques, we derive the properties of the phonon fluxes emitted when the condensate flow crosses the sound speed. Our analysis is based on the Bogoliubov-de Gennes (BdG) equation, without introducing any (hydrodynamical) approximation. More specifically, we consider one dimensional stationary condensates which contain one sonic horizon (black or white), surrounded on either side by two infinite asymptotically homogeneous regions. In this case, at fixed conserved frequency  $|\omega|$ , three types of asymptotic phonons exist, and a complete description of their scattering is given in terms of a  $3 \times 3$  Bogoliubov transformation.

In stationary Gaussian states (e.g. vacuum and thermal state), the physical predictions encoded in this scattering are all contained in two groups of expectation values: firstly, three occupation numbers, i.e., one for each type of emitted phonons ( $\bar{n}_\omega^i = \langle a_{\omega,i}^{out\dagger} a_{\omega,i}^{out} \rangle$ ,  $i = 1, 2, 3$ ), and secondly, three interference terms such as  $\langle a_{\omega,i}^{out} a_{\omega,j}^{out} \rangle$  with  $i \neq j$ . As we shall see, the latter determine the long distance correlations of the density-density correlation function. In this study, we were motivated by the recent work [10, 11] where a distinct pattern of

correlations was “numerically observed” when the condensate velocity crosses the speed of sound. In what follows, we shall explain both the properties of this pattern, and also why, when taking into account the condensate temperature, the initial distributions of phonons tend to hide the black hole radiation in the occupation numbers whereas, at the same time, they reinforce the correlations pattern without affecting its spatial properties. This confirms that this pattern offers a neat signature of the Hawking effect.

In Sec. II, we present our settings and derive the mode equation for the phonon field in one dimensional stationary condensates. To be general, we consider nonhomogeneous condensates whose sonic horizon can be either due to the velocity flow  $v(x)$ , or to a varying sound speed  $c(x)$ , or to a combination of these two. We shall later see that some fluxes properties (such as the backscattering mixing left- and right-moving phonons) crucially depend on the particular combination which is realized.

In Sec. III, we analyze the mode equation, we identify the combinations of solutions which describe initial and final asymptotic phonons, and relate them by the aforementioned  $3 \times 3$  Bogoliubov transformation. We explain under which circumstances this scattering induces a spontaneous and steady production of pairs of phonons, and how it governs both local (e.g. occupation numbers) and nonlocal (density-density correlations) observables. This is carried out twice, without and with an initial temperature.

In Sec. IV, we numerically solve the mode equation and obtain the spectral properties of the occupation numbers of the three types of phonons.

A word about the presentation: we have tried to be self-contained, something which at times renders the discussions rather lengthy, but hopefully will allow a broad audience to follow easily. We also mention that many of the results of this paper –among which those concerning the Bogoliubov description of the phonon field in a stationary condensate– were presented in the meeting “Towards the observation of Hawking radiation in condensed matter systems” (<http://www.uv.es/workshopEHR/>) held at IFIC in Valencia in February 2009.

## II. THE SETTINGS

### A. Dilute gases

We give here the basic ingredients which describe the condensates and their linearized perturbations. The reader is referred to the review [9] for more details.

In a second quantized formalism, the set of atoms is described by a field operator  $\Psi(t, \mathbf{x})$  which annihilates an atom at  $t, \mathbf{x}$ , and which obeys the equal time commutator

$$[\Psi(t, \mathbf{x}), \Psi^\dagger(t, \mathbf{x}')] = \delta^3(\mathbf{x} - \mathbf{x}'). \quad (1)$$

The time evolution of  $\Psi$  is given by the Heisenberg equation

$$i\hbar \partial_t \Psi(t, \mathbf{x}) = [\Psi(t, \mathbf{x}), H], \quad (2)$$

where the Hamiltonian is

$$H = \int d^3x \left\{ \frac{\hbar^2}{2m} \nabla_{\mathbf{x}} \Psi^\dagger \nabla_{\mathbf{x}} \Psi + V \Psi^\dagger \Psi + \frac{g}{2} \Psi^\dagger \Psi^\dagger \Psi \Psi \right\}. \quad (3)$$

In this expression,  $m$  is the mass of the atoms,  $V$  the external potential, and  $g$  the effective coupling constant, which describes the scattering of atoms by a local term.

At sufficiently low temperature, of the order of 300 nK for  $10^4$  atoms, a large fraction of the atoms condensates in a common state. To separate the condensate from its perturbations, the field operator is decomposed into a  $c$ -number wave describing the condensed atoms,  $\Psi_0$ , and a fluctuation:

$$\Psi = \Psi_0 + \tilde{\phi}. \quad (4)$$

In the mean field approximation,  $\Psi_0$  satisfies the nonlinear Gross-Pitaevskii (GP) equation

$$i\partial_t \Psi_0 = [T + V + g\rho_0] \Psi_0, \quad (5)$$

where the kinetic operator is  $T = -\hbar^2 \nabla_{\mathbf{x}}^2 / 2m$ . This equation guarantees that  $\rho_0 = |\Psi_0|^2$  obeys the continuity equation:  $\partial_t \rho_0 + \text{div}(\rho_0 \mathbf{v}) = 0$ , where  $\mathbf{v}$  is the condensate velocity.

### B. Stationary condensates

In the general case,  $V$  and  $g$  depend on both  $\mathbf{x}$  and  $t$ . In the body of this work we shall only consider stationary cases. In Appendix A, the time-dependent case is presented. Before

proceeding, let us make clear that stationarity, here, means that there is a Galilean frame (that needs not coincide with the lab frame) in which  $V, g$  and therefore  $\rho_0$  only depend on  $\mathbf{x}$ . From now on we work in this “preferred” frame.

In this frame, the condensate wave function has the form

$$\Psi_0(t, \mathbf{x}) = e^{-i\mu t/\hbar} \times \sqrt{\rho_0(\mathbf{x})} e^{iW_0(\mathbf{x})}, \quad (6)$$

where  $\rho_0(\mathbf{x})$  gives the (mean) density of condensed atoms,  $\mu$  is the chemical potential, and  $\mathbf{k}_0(x) = \partial_{\mathbf{x}} W_0$  is the condensate wave vector.

In the sequel, we shall work with one dimensional condensates. This means that the transverse excitations have energies much higher than the longitudinal ones, and than the interaction energy  $g\rho_0$ . The transverse excitations can therefore be ignored at sufficiently low energies. This simplifying hypothesis can be relaxed without significantly modifying the forthcoming treatment.

For one dimensional stationary condensates, the continuity equation reduces to

$$\rho_0(x)v(x) = \text{cst.} \quad (7)$$

where  $v(x) = \hbar k_0(x)/m$  is the velocity of the condensate, and where  $x$  is the longitudinal coordinate. Plugging Eq. (6) in Eq. (5) gives

$$\mu = \left[ \frac{mv^2(x)}{2} + \rho_0^{-1/2} T \rho_0^{1/2} + V(x) + g(x)\rho_0(x) \right]. \quad (8)$$

Because of Eq. (7), the nonhomogeneity of the background is characterized by two independent functions that can be taken to be  $v(x)$  and  $g(x)$ . As we shall see below the mode equation of density fluctuations depend on  $v(x)$  and on the  $x$ -dependent speed of sound

$$c^2(x) = g(x) \frac{\rho_0(x)}{m}. \quad (9)$$

In what follows we shall thus treat  $v$  and  $c$  as two independent functions.

### C. Bogoliubov-de Gennes equation

Inserting Eq. (4) in Eq. (2), and linearizing the equation in  $\tilde{\phi}$ , one gets

$$i\hbar\partial_t\tilde{\phi} = [T + V + 2g|\Psi_0|^2] \tilde{\phi} + g\Psi_0^2 \tilde{\phi}^\dagger. \quad (10)$$

Given the structure of this equation and Eq. (8), we found that it is mathematically more convenient to work with relative (dimensionless) fluctuations  $\phi$  defined by

$$\Psi = \Psi_0 (1 + \phi). \quad (11)$$

Then using Eqs. (6, 9), one gets

$$i\hbar\partial_t\phi = \left[ T - \hbar^2 \frac{\partial_x(\ln \Psi_0)}{m} \partial_x \right] \phi + mc^2 [\phi + \phi^\dagger]. \quad (12)$$

When dealing with stationary condensates, the field operator can be written as a superposition of solutions of the form

$$\phi_\omega(t, x) = a_\omega e^{-i\omega t} \phi_\omega(x) + a_\omega^\dagger (e^{-i\omega t} \varphi_\omega(x))^*, \quad (13)$$

where  $a_\omega, a_\omega^\dagger$  are phonon annihilation and creation operators. In the next section we shall study the normalization of the doublets  $W_\omega = (\phi_\omega, \varphi_\omega)$ , and their completeness in supersonic flows. In what follows we focus on the equations they obey.

Inserting Eq. (13) in Eq. (12), and taking the commutator of Eq. (12) with  $a_\omega$  and  $a_\omega^\dagger$  yields the equation obeyed by the doublet:

$$\begin{aligned} [\hbar(\omega + iv\partial_x) - T_\rho - mc^2] \phi_\omega &= mc^2 \varphi_\omega, \\ [-\hbar(\omega + iv\partial_x) - T_\rho - mc^2] \varphi_\omega &= mc^2 \phi_\omega. \end{aligned} \quad (14)$$

To simplify the equations, we have introduced the “dressed” kinetic operator

$$T_\rho = -\frac{\hbar^2}{2m\rho_0} \partial_x \rho_0 \partial_x = -\hbar^2 \frac{v}{2m} \partial_x \frac{1}{v} \partial_x. \quad (15)$$

The  $2 \times 2$  system (14) is the mode equation we shall study. It follows from the hypothesis that the condensate is stationary, and contains no approximation besides those involved in the BdG equation [9, 12]. In the sequel, we shall analyze its solutions when the profile  $c(x) + v(x)$  describes a black hole horizon. In particular, we shall identify the initial and final sets of normalized doublets  $W_\omega^{(i)}$  associated with the asymptotic solutions. We shall then numerically integrate Eq. (14) to obtain the coefficients of the transformation relating these two sets since they determine the spectral properties of the produced phonon pairs.

From an algebraic point of view, Eq. (14) closes this section. In what follows we discuss its properties and its relations with other dispersive models which have been recently studied.

## D. Additional remarks

### 1. Eikonal approximation and importance of ordering

To eliminate  $\varphi_\omega$  and obtain an equation for  $\phi_\omega$ , we divide the first line of Eq. (14) by  $c^2$  and act on the resulting equation with the operator in bracket of the second line. We obtain

$$[-\hbar(\omega + iv\partial_x) - T_\rho - mc^2] \frac{1}{c^2} [\hbar(\omega + iv\partial_x) - T_\rho - mc^2] \phi_\omega = m^2 c^2 \phi_\omega, \quad (16)$$

which can be simplified as

$$\left\{ [\hbar(\omega + iv\partial_x) + T_\rho] \frac{1}{c^2} [-\hbar(\omega + iv\partial_x) + T_\rho] - \hbar^2 v \partial_x \frac{1}{v} \partial_x \right\} \phi_\omega = 0. \quad (17)$$

One verifies that  $\varphi_{-\omega}^*$  obeys the same equation.

We first notice that

$$c^2 [\hbar(\omega + iv\partial_x) + T_\rho] \frac{1}{c^2} = [\hbar(\omega + iv\partial_x) + T_\rho] + c^2 \left[ (i\hbar v \partial_x + T_\rho), \frac{1}{c^2} \right]. \quad (18)$$

This makes explicit that the spatial gradient of  $c^2$  affects Eq. (17) only through a commutator. At this point, to better understand the system under study, it is of interest to give the equation for  $\varphi_\omega$ , the other mode of Eq. (13). One finds

$$\left\{ [-\hbar(\omega + iv\partial_x) + T_\rho] \frac{1}{c^2} [\hbar(\omega + iv\partial_x) + T_\rho] - \hbar^2 v \partial_x \frac{1}{v} \partial_x \right\} \varphi_\omega = 0. \quad (19)$$

The only differences between the equations for  $\phi_\omega$  and for  $\varphi_\omega$  come from the sign of the commutator between  $v\partial_x$  and  $c^{-2}$ . When this commutator is neglected,  $\phi_\omega$  and  $\varphi_\omega$  thus obey the same equation.

When working to leading order in a WKB (or eikonal) approximation, i.e., inserting  $\phi_\omega \sim e^{i\int dx k_\omega}$  in Eq. (17) (or inserting  $\varphi_\omega \sim e^{i\int dx k_\omega}$  in Eq. (19)), gives the dispersion relation in a moving fluid of velocity  $v$ ,

$$(\omega - kv)^2 = \Omega^2 = k^2 c^2 + \frac{\hbar^2 k^4}{4m^2} = c^2 k^2 \left( 1 + \frac{\xi^2 k^2}{2} \right), \quad (20)$$

where  $\xi = \hbar/\sqrt{2}mc$  is the healing length. We recover the quartic dispersion relation between the frequency in the comoving frame  $\Omega = (\omega - kv)$ , and the wave vector  $k$ .

It should be noticed that in a stationary nonhomogeneous flow,  $\Omega$  and  $k$  depend on  $x$  through  $v(x)$ , whereas the frequency  $\omega$  is constant. Remember that  $\omega$  is not necessarily

the lab frequency, because, as explained, it is defined in the frame in which the condensate quantities only depend on  $x$ .

Returning to Eq. (17), it is clear that its role is to fix the exact properties of the ODE obeyed by  $\phi_\omega$ . These properties could not have been inferred starting from Eq. (20), and applying the substitution  $k \rightarrow -i\partial_x$ , because this naive rule could neither predict the ordering of  $T$ ,  $v(x)$  and  $c^2(x)$  found in Eq. (17), nor the different one found in Eq. (19).

## 2. Hydrodynamical limit and Euler mode equation

For long wavelengths with respect to the healing length  $\xi$ , i.e., in the hydrodynamical (dispersionless) limit  $\xi \rightarrow 0$ , one can drop the two operators  $T_\rho$  in Eq. (17). Then Eq. (17) reduces to the Eulerian mode equation which describes sound waves in a moving fluid, and this with the correct nontrivial ordering of  $T$ ,  $v(x)$  and  $c^2(x)$ . Let us verify this.

The Eulerian action is usually written in terms of the velocity potential  $\psi$ , related to the velocity fluctuation by  $\delta v = \partial_x \psi$ , see e.g. [13]. To make contact between  $\psi$  and the  $\phi$  field, one should compare the fluctuations of  $\Psi$  described as in Eq. (11) to those written as

$$\delta\Psi = \delta(\rho^{1/2} e^{iW}) = \Psi_0 \left( \frac{\delta\rho}{2\rho_0} + i\delta W \right) = \Psi_0 \phi. \quad (21)$$

Using  $\delta v = \frac{\hbar}{m} \partial_x \delta W = \partial_x \psi$ , one obtains

$$\begin{aligned} \phi + \phi^\dagger &= \frac{\delta\rho}{\rho_0}, \\ \frac{\phi - \phi^\dagger}{2i} &= \theta = \delta W = \frac{m}{\hbar} \psi. \end{aligned} \quad (22)$$

Using the phase fluctuation  $\theta = m\psi/\hbar$  rather than  $\psi$  itself, the Euler action is

$$S_E = \frac{\hbar}{2m} \int dt dx \rho_0 \left\{ \frac{1}{c^2} [(\partial_t + v\partial_x)\theta]^2 - (\partial_x\theta)^2 \right\}. \quad (23)$$

Then, using the continuity equation, the mode equation reads

$$\left\{ \left[ (\partial_t + v\partial_x) \frac{1}{c^2} (\partial_t + v\partial_x) \right] - \frac{1}{\rho_0} \partial_x \rho_0 \partial_x \right\} \theta = 0. \quad (24)$$

When working at fixed  $\omega = i\partial_t$ , and using  $v\rho_0 = \text{cst.}$ , as announced, one recovers the dispersionless limit of Eq. (17) obtained by taking the limit  $T_\rho \rightarrow 0$ .

Notice that Eq. (24) is a generalization of the (dispersionless limit of the) mode equation which has been generally studied in the literature, see Refs. [3, 4, 5, 13, 14]. In those

references, the equation also followed from Eq. (23), but with the extra hypothesis that both  $c$  and  $\rho_0$  can be approximated by constants, in which case one recovers the massless relativistic 2D mode equation.

### 3. Link with Unruh's dispersive models

It is worth noticing that the dispersive properties of the phonons come through the two operators  $T_\rho$  in Eq. (17). This is not what we would have obtained had we used the rules of [3] with a quartic supersonic dispersion. Indeed, the Eulerian action supplemented by a quartic term ( $k^4/\Lambda^2$ ) is

$$S_\Lambda = \frac{\hbar}{2m} \int dt dx \rho_0 \left\{ \frac{1}{c^2} [(\partial_t + v\partial_x)\theta]^2 - (\partial_x\theta)^2 + \frac{1}{\Lambda^2} (\partial_x^2\theta)^2 \right\}, \quad (25)$$

and the corresponding mode equation reads, in a stationary condensate and at fixed  $\omega$ ,

$$\left\{ \left[ (\omega + iv\partial_x) \frac{1}{c^2} (\omega + iv\partial_x) \right] - v \partial_x \frac{1}{v} \partial_x + \frac{v}{\Lambda^2} \partial_x^2 \frac{1}{v} \partial_x^2 \right\} \theta_\omega = 0. \quad (26)$$

In nonhomogeneous situations, the quartic term encoding the dispersion differs from that of Eq. (17), which means that  $\theta_\omega(x)$  will differ from  $\phi_\omega(x)$  in any nontrivial background.

Finally, it is also worth noticing that Eq. (17) *can* be obtained from an action for a single field with a quadratic kinetic term, and which generalizes the Euler action:

$$S_\phi = \frac{\hbar}{2m} \int dt dx \rho_0 \left\{ \frac{1}{c^2} \left[ \left( \partial_t + v\partial_x + i \frac{T_\rho}{\hbar} \right) \phi \right]^2 - (\partial_x\phi)^2 \right\}. \quad (27)$$

This action can be obtained from  $S = \int dt d^3x (i\Psi\partial_t\Psi^* - H)$ , where  $H$  is given in Eq. (3), using Eq. (11), keeping all quadratic terms in  $\phi, \phi^*$ , and using Eq. (12) to eliminate  $\phi^*$  in favor of  $\phi$ .

The conjugate momentum of  $\psi$  is rather unusual

$$\pi = \frac{\hbar}{m} \frac{\rho_0}{c^2} \left( \partial_t + v\partial_x + i \frac{T_\rho}{\hbar} \right) \psi. \quad (28)$$

It should be used in the equal time commutator  $[\psi(x), \pi(y)] = i\hbar\delta(x-y)$ , and it enters into the conserved scalar product

$$(\psi_2, \psi_1) = i \int dx (\psi_2^* \pi_1 - \psi_1 \pi_2^*). \quad (29)$$

It is not clear whether this alternative way of describing the phonon field presents any advantage over the original version of Eq. (14). It could be useful to study how dispersion affects the analogy with gravitational systems. [15, 16]

### E. Background profile and black hole trajectories

To choose the profiles  $c(x)$  and  $v(x)$  which give rise to a black hole horizon, we can refer to the gravitational analogy [6], or directly analyze the characteristics of Eq. (17). Adopting the second, perhaps more intrinsic, approach, we perform a long wavelength approximation to Eq. (17), i.e., we drop the  $T_\rho$  terms, and consider the semi-classical WKB solutions of the resulting quadratic equation. In this approximation, right ( $u$ ) and left ( $v$ ) moving solutions decouple and are governed by an  $x$ -dependent momentum  $k_\omega^u$ , and  $k_\omega^v$  respectively. These momenta are given by

$$\omega - k_\omega v(x) = \pm k_\omega c(x), \quad (30)$$

where the  $+$  ( $-$ ) sign governs  $k_\omega^u$  ( $k_\omega^v$ ), and where  $c(x) > 0$  by convention.

The behavior that is peculiar to horizons can be obtained in two cases depending on whether it is  $c + v$  (or  $c - v$ ) that crosses zero. Assuming it is  $c + v$ , the condensate flows to the left, i.e.,  $v < 0$ , and the modes which experience the horizon are the right moving ones. We further require that  $c + v$  smoothly crosses zero, i.e., that the following expansion is valid in a finite range:

$$c + v = \kappa x + O(x^2). \quad (31)$$

We have set to  $x = 0$  the location of the sonic horizon, and we call the *near horizon region*, the range of  $x$  where the neglect of nonlinear terms in Eq. (31) is valid.

To get the space-time trajectories associated with Eq. (30) we consider the Hamilton-Jacobi equations ( $dx/dt = \partial\omega/\partial k$ ,  $dk/dt = -\partial\omega/\partial x$ ). These trajectories give the locus of constructive interference when considering wave-packets. In the near horizon region, we get for the right movers

$$\begin{aligned} k &= k_0 e^{-\kappa t}, \\ x &= x_0 e^{\kappa t}, \end{aligned} \quad (32)$$

since  $\omega = k\kappa x = \text{constant}$ . By definition, whenever such equations are obtained with  $\kappa > 0$ , one is dealing with a black hole horizon. When instead  $\kappa < 0$ , the structure of the trajectories is that of a white hole. The two cases are related by a time reversal symmetry, see Appendix B. It should be noticed that in both cases the relevant quantity is the “decay rate”  $\kappa$ , given by the gradient

$$\kappa = \left. \frac{d(c + v)}{dx} \right|_{\text{horizon}}, \quad (33)$$

evaluated at the sonic horizon  $c + v = 0$ . (In the general relativistic jargon it is called the “surface gravity” (when multiplied by  $c$ ). It plays a crucial role in the laws of black hole thermodynamics [17, 18], and it fixes the temperature of black hole radiation when using relativistic fields [19].) One should also point out that the left movers, the  $v$ -modes, are hardly affected by the horizon since  $-c + v \sim 2v - \kappa x$  can be, to a good approximation, treated as a constant in the near horizon region.

In the sequel, we shall work with

$$c(x) + v(x) = c_0 D \times \text{sign}(x) \tanh^{1/n} \left[ \left( \frac{|\kappa x|}{D c_0} \right)^n \right]. \quad (34)$$

The parameter  $1 > D > 0$  determines the size of the near horizon region, namely  $|\Delta x| = D c_0 / \kappa$ . As we shall see, it plays a critical role in the deviations with respect to the standard relativistic fluxes. The power  $n$  controls the sharpness of the transition from the linear near horizon behavior of  $c$  to the asymptotic flat regions on either side. For  $n \rightarrow \infty$ , the transition becomes sharp. As discussed in [5, 14], sharp transitions give rise to nonadiabatic effects which produce superimposed oscillations on the fluxes. In this paper, we shall work with  $n$  equal to 2, and we refer to [14] for more details about this aspect.

Given that the left-moving  $v$ -modes “see” the combination  $c - v$ , and are coupled to the  $u$ -modes, we need to specify both  $v$  and  $c$ , and not only the combination of Eq. (34) which fixes the surface gravity. To this end, we introduce a new parameter  $q$  which specifies how  $c + v$  is shared between  $c$  and  $v$ :

$$\begin{aligned} c(x) &= c_0 + (1 - q) (c(x) + v(x)), \\ v(x) &= -c_0 + q (c(x) + v(x)). \end{aligned} \quad (35)$$

In this parameterization  $v + c_0$  and  $c - c_0$  have the same profile, and the value of  $\kappa$  is independent of  $q$ . For  $q = 1$  (resp.  $q = 0$ ) the hole is purely due to the gradient of  $v$  (resp.  $c$ ).

### III. THEORETICAL ANALYSIS

To prepare the numerical analysis of the solutions of Eq. (14), it is worth studying in detail the structure of these modes, and the Bogoliubov transformation relating the two asymptotic mode bases.

We remind the reader that in the absence of dispersion, and for a relativistic 2D massless field, the Bogoliubov transformation induced by propagating the field in Eq. (34) is particularly simple because, at fixed  $\omega$ , one only has two types of modes, left and right movers, and because these two sectors completely decouple, thanks to the conformal invariance, see e.g. [20]. When dealing with Eq. (14) (or equivalently with Eq. (17)), one faces two novelties. First, at fixed  $\omega$  four independent solutions now exist, and secondly, the left-right decoupling is no longer exact, and this even in the dispersionless limit  $m \rightarrow \infty$  to Eq. (17).

### A. Asymptotic solutions

In Eq. (34),  $c+v$  is asymptotically constant in the regions  $|\kappa x| \gg Dc_0$ , where the general solution of Eq. (17) is thus a superposition of plane waves  $e^{ikx}$  with constant amplitudes. To characterize the solution, we thus need the roots  $k(\omega)$ . Owing to the nonlinear character of the dispersion relation, in addition to the (physical) oscillatory modes possessing a real wave vector, a growing and a decaying mode exist, governed by complex values of  $k$ . The asymptotic roots are solutions of

$$(\omega - v_{\pm}k)^2 = c_{\pm}^2 k^2 + \frac{\hbar^2 k^4}{4m^2} = \Omega_{\pm}^2(k). \quad (36)$$

For  $\omega > 0$ , in the subsonic region  $c_+ < |v_+|$ , there is one real root  $k_{\omega}^u > 0$  which corresponds to a right mover and another real root  $k_{\omega}^v < 0$  which describes a left mover, see Fig. 1, where the two extreme cases  $q = 1$  (left plot) and  $q = 0$  (right plot) are represented. There is also a pair of complex conjugated roots (since the equation is real). One thus has a root with a negative (resp. positive) imaginary part which corresponds to a growing (resp. decaying) mode to the right.

On the left of the horizon, in the supersonic region  $c_- > |v_-|$ , for  $\omega$  larger than a critical frequency  $\omega_{\max}$  (we shall compute its value below) there are only two real roots, as in a subsonic flow. Instead for  $0 < \omega < \omega_{\max}$  four real roots exist. This doubling of the number of real roots is illustrated in Fig. 2. Thus the pair of growing and decaying modes which existed in the subsonic flow has been replaced by a couple of oscillatory modes. Such replacements of pairs of modes is a generic feature of QFT in external fields, see [21]. In BEC it will occur at all horizons, for both black and white holes.

Given that there are 4 roots, the general solution of Eq. (17) will be a superposition of

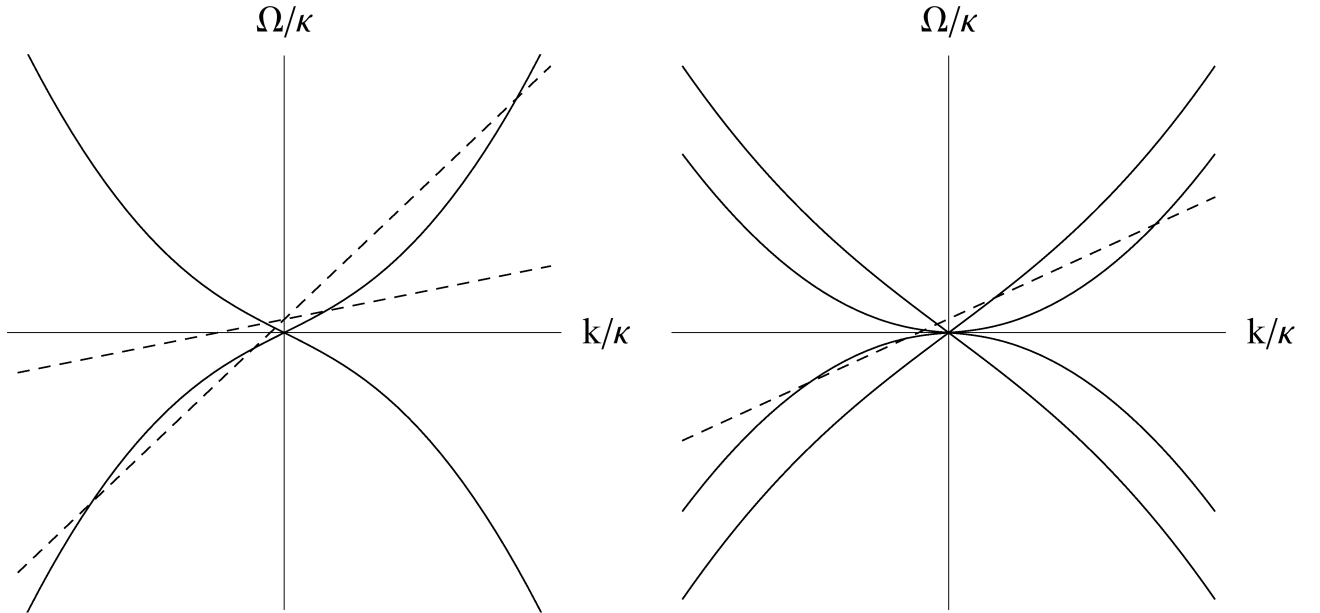


Figure 1: Graphical resolution of the dispersion relation Eq. (36), for  $q = 1$  (left plot), and  $q = 0$  (rightplot). The straight lines represent  $\omega - v_{\pm}k$  and the curves represent  $\Omega_{\pm}(k)$ . The solutions  $k(\omega)$  are given by the abscissa of their intersections.

4 modes. However, when considering the Fourier transform of the field operator  $\phi$ , only a subclass should be used. Namely, in infinite condensates, one should only keep modes that are asymptotically bounded for both  $x \rightarrow \pm\infty$ . Moreover, this subclass is *complete* in a precise sense we recall below. To establish the completeness of the mode basis we first need to compute the value of  $\omega_{\max}$  which, as we shall later see, will cutoff Hawking radiation.

### B. Maximal frequency $\omega_{\max}$

The maximal frequency  $\omega_{\max}$  is the value of  $\omega$  where the two extra real roots merge into each other. It is thus reached when the straight line  $\omega - c_- k$  is tangent to the negative branch of the dispersion relation  $-\Omega_-(k)$ , or equally when  $-|\omega| - c_- k$  is tangent to  $\Omega_-(k)$ , the positive root of Eq. (36) evaluated on the supersonic region on the left of the horizon. The corresponding value of  $k_{\max}$  is

$$k_{\max} = \frac{1}{\sqrt{2}} \frac{m}{\hbar} \sqrt{v_-^2 - 4c_-^2 + |v_-| \sqrt{v_-^2 + 8c_-^2}}. \quad (37)$$

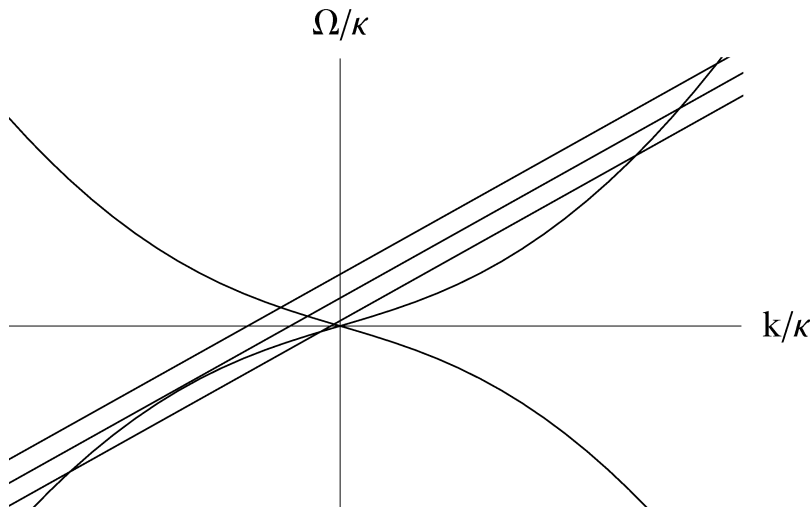


Figure 2: Graphical resolution of the dispersion relation in the supersonic region for three values of  $\omega$ :  $0 < \omega < \omega_{\max}$ ,  $\omega = \omega_{\max}$  and  $\omega > \omega_{\max}$ .

Then  $\omega_{\max}$  is obtained by replacing  $k$  by  $k_{\max}$  in Eq. (36). Using Eq. (34) and Eq. (35), it is thus of the form

$$\omega_{\max} = \Lambda \times f(D, q), \quad (38)$$

where the “healing” frequency  $\Lambda$  is related to the central value of the healing length computed with  $c_0$

$$\xi_0 = \frac{\hbar}{\sqrt{2}mc_0}, \quad (39)$$

by  $\Lambda = \sqrt{2}c_0/\xi_0$ . (The prefactor  $\sqrt{2}$  has been added so that the quartic term in the dispersion relation Eq. (36) be equal to  $k^4c_0^2/\Lambda^2$ .) In what follows,  $\Lambda$  (or the adimensional  $\lambda = \Lambda/\kappa$ ) is referred to as the dispersion scale and is used to characterize the importance of dispersion.

For  $D \ll 1$ , one has  $f(D, q) \propto D^{3/2}$ . This means that  $\omega_{\max}$  can be much smaller than  $\Lambda$ . The contours of constant  $\omega_{\max}/\kappa$  in the  $(D, \lambda)$ -plane are shown in Fig. 3, for  $q = 0$  and  $q = 1$ . One sees that  $q$  has only little influence on the value of  $\omega_{\max}/\kappa$  when this latter is small, but the effect becomes significant for larger values. The physical consequences of this shall be seen in Sec. IV B 3.

### C. Mode Orthonormality and Mode Completeness

To proceed to the canonical quantization of  $\phi$ , one needs a mode basis which is orthonormal and complete. The orthonormality is defined with respect to the conserved scalar

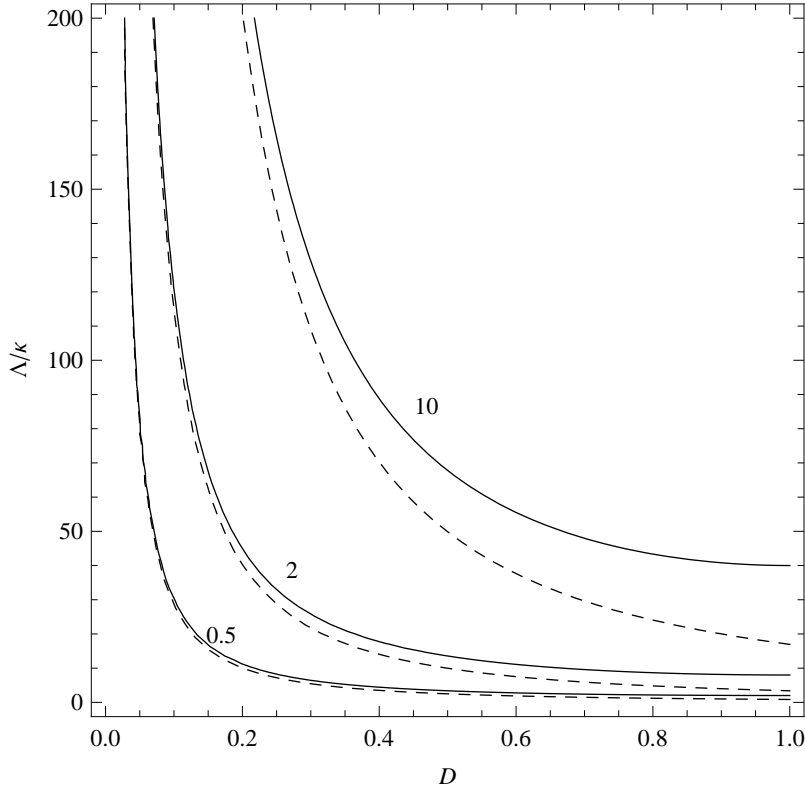


Figure 3: Contours of constant  $\omega_{\max}/\kappa$  in the  $(D, \lambda)$  plane, for  $q = 0$  (solid lines) and  $q = 1$  (dashed lines).

product on the space of the solutions of Eq. (14). In terms of the doublet  $W_i = (\phi_i, \varphi_i)$ , the scalar product takes the form

$$(W_1, W_2) = \int_{-\infty}^{\infty} dx \rho_0(x) [\phi_1^* \phi_2 - \varphi_1^* \varphi_2]. \quad (40)$$

The presence of  $\rho_0$  in this product follows from the use of the rescaled fluctuations defined in Eq. (11). (This  $x$ -dependent measure induces no difficulty, and moreover, if one wishes, one can get rid of it by using the nonCartesian coordinate  $y$  defined by  $dy = dx\rho_0(x)$ .)

When the condensate is homogeneous the quantization is rather straightforward. However, when the flow  $c+v$  possesses a horizon, the situation is more subtle. Therefore, before considering the inhomogeneous backgrounds of Eq. (34), let us quantize  $\phi$  when  $c$  and  $v$  are constant both in space and time.

1. *Homogeneous condensates,  $k$ -representation*

In homogeneous condensates, it is appropriate to exploit the (spatial) homogeneity and express the field in terms of exponentials  $e^{ikx}$  and creation/destruction operators labeled by the (real) wave-vector  $k$ ,

$$\hat{\phi} = \int_{-\infty}^{\infty} dk \left[ \hat{a}_k \phi_k + \hat{a}_k^\dagger \varphi_k^* \right], \quad (41)$$

where

$$\phi_k(t, x) = \frac{e^{-i\omega_k t + ikx}}{\sqrt{2\pi\rho_0}} \mathbf{u}_k, \quad \varphi_k(t, x) = \frac{e^{-i\omega_k t + ikx}}{\sqrt{2\pi\rho_0}} \mathbf{v}_k, \quad (42)$$

and where  $\omega_k$  is the solution of Eq. (36).

Using these expressions, one verifies that the orthonormality conditions

$$\begin{aligned} (W_k, W_{k'}) &= \delta(k - k'), \\ (\bar{W}_k, W_{k'}) &= 0, \end{aligned} \quad (43)$$

are satisfied, where the “bar” doublet obtained from  $W_k = (\phi_k, \varphi_k)$  is  $\bar{W}_k = (\varphi_k^*, \phi_k^*)$ , and where the amplitudes  $\mathbf{u}_k, \mathbf{v}_k$  have their standard expression, irrespectively of the (sub- or supersonic) value of the condensate velocity  $v$ . Explicitly, using Eq. (14) and Eq. (20), one obtains

$$\begin{aligned} \mathbf{v}_k &= D_k \mathbf{u}_k, \quad |\mathbf{u}_k|^2 - |\mathbf{v}_k|^2 = 1, \\ D_k &= \left( \hbar \sqrt{c^2 k^2 + \frac{\hbar^2 k^4}{4m^2}} - \left( mc^2 + \frac{\hbar^2 k^2}{2m} \right) \right) / (mc^2). \end{aligned} \quad (44)$$

The fact that  $D_k$  is independent of the condensate velocity  $v$  follows from Galilean invariance, the condensate being homogeneous. Indeed, in the coordinates  $t_c, x_c$  comoving with the fluid, related to the coordinates  $t, x$  by  $t_c = t, x_c = x - vt$ , the 2D wave vector of components  $(\omega_k, k)$  in the  $t, x$  system has comoving components  $(\Omega_k = \omega_k - vk, k)$  where all reference to  $v$  drops out when using  $k$  to label modes, as can be seen from Eq. (20).

The operators  $\hat{a}_k, \hat{a}_k^\dagger$  obey the usual bosonic commutation relation  $[\hat{a}_k, \hat{a}_{k'}^\dagger] = \delta(k - k')$ . The relationships between mode doublets  $W_k$  and these operators follow from

$$\begin{aligned} \hat{a}_k &= (W_k, \hat{W}), \\ \hat{a}_k^\dagger &= -(\bar{W}_k, \hat{W}), \end{aligned} \quad (45)$$

where the doublet operator is  $\hat{W} = (\hat{\phi}, \hat{\phi}^\dagger)$ .

In this  $k$ -representation, one can also easily verify that the mode basis is complete. That is, starting with the commutators  $[\hat{a}_k, \hat{a}_{k'}^\dagger] = \delta(k - k')$  and the doublets  $W_k$ , making use of the completeness (in the sense of Fourier analysis) of the exponentials  $e^{ikx}$  with  $k$  real from  $[-\infty, \infty]$ , and using that  $D_k = D_{-k}$  (which is a necessary condition) one verifies that the equal time commutator

$$[\phi(t, x), \phi^\dagger(t, x')] = \frac{1}{\rho_0} \delta(x - x'), \quad (46)$$

is satisfied, again irrespectively of the value of the condensate velocity  $v$ .

The lesson one can draw from this is that, in homogeneous condensate flows, when using the conserved frequency  $\omega$  instead of  $k$  to label modes and operators, one should discard the growing and the decaying solutions of Eq. (17) because they are not bounded asymptotically (in space). Unlike the oscillatory plane waves, they cannot be reached in a limiting procedure starting with square integrable functions, and thus do not belong to the “complete” set of solutions one should use in field operators.

## 2. Homogeneous condensates, $\omega$ -representation

When considering nonhomogeneous but stationary flows, one must use the conserved frequency  $\omega$  in the place of the wave vector  $k$  to label modes and operators. Then one notices that the re-arrangement of the various terms according to the value of  $\omega$  strongly differs according to the sub- or supersonic character of the flow. As a preliminary step, we consider the description of the field operator in the  $\omega$ -representation in sub- and supersonic homogeneous flows.

Let us first consider a homogeneous subsonic flow. In this case only two real roots  $k(\omega)$  exist. Given that  $dk/d\omega$  does not cross zero neither for right nor for left movers, one can re-express the integral over wave vectors in Eq. (41) into an integral over frequencies of the sum of the right and left movers, i.e.,

$$\phi(t, x) = \int_0^\infty d\omega \left[ e^{-i\omega t} \hat{\phi}_\omega(x) + e^{+i\omega t} \hat{\phi}_\omega^\dagger(x) \right], \quad (47)$$

where

$$\begin{aligned} \hat{\phi}_\omega(x) &= \hat{a}_\omega^u \phi_\omega^u(x) + \hat{a}_\omega^v \phi_\omega^v(x), \\ \hat{\phi}_\omega^\dagger(x) &= \hat{a}_\omega^u \varphi_\omega^u(x) + \hat{a}_\omega^v \varphi_\omega^v(x), \end{aligned} \quad (48)$$

The rescaled modes and operators are  $\phi_\omega = \phi_k \sqrt{dk/d\omega}$ , and  $\hat{a}_\omega = \hat{a}_k \sqrt{dk/d\omega}$ . One easily verifies that the factors  $\sqrt{dk/d\omega}$  guarantee that all  $\delta(k-k')$  obtained in the former subsection are consistently replaced by  $\delta(\omega-\omega')$ . That is, the operators  $\hat{a}_\omega, \hat{a}_\omega^\dagger$  obey  $[\hat{a}_\omega, \hat{a}_{\omega'}^\dagger] = \delta(\omega-\omega')$ . Similarly the modes  $\phi_\omega^u$  and  $\phi_\omega^v$  are orthogonal to each other, and possess unit positive norm (in the sense of a Dirac distribution  $\delta(\omega-\omega')$ ).

We now consider a homogeneous supersonic flow. The situation is trickier because  $dk/d\omega$  flips sign in the right moving sector. Starting again from Eq. (41) one decomposes, as in Eq. (47), the field as an integral over  $\omega$  of a sum of right and left moving modes. When considering the left moving sector in left moving flow  $v < 0$ , nothing changes when the flow is supersonic because  $dk/d\omega$  still does not cross zero. Therefore, as in subsonic flows, all left moving (positive norm) modes can still be monotonically labelled by  $\omega$  belonging to  $[0, \infty]$ .

The same is no longer true for the right moving sector. In fact, the integral  $\int_0^\infty dk$  splits into an integral over  $\omega$  belonging to  $[0, \infty]$  plus another piece over negative frequencies belonging to  $[-\omega_{\max}, 0]$ . In addition, for a given value of  $\omega < 0$  in this interval, two real roots  $k^u(\omega) > 0$  exist. It ends when the two roots merge into each other when  $-\omega_{\max}$  is reached.

Thus, for  $\omega > \omega_{\max}$ , one has only one (positive norm)  $u$ -root and  $\hat{\phi}_\omega, \hat{\varphi}_\omega$  read as in Eq. (48). Instead, when  $0 < \omega < \omega_{\max}$ , three real roots exist: the continuation (in  $\omega$ ) of the former positive norm one, and two new roots with negative  $\Omega$ , see Fig. 2. In this case, the  $\pm\omega$  Fourier transform of  $\phi$  must be decomposed as

$$\begin{aligned} \int \frac{dt}{2\pi} e^{i\omega t} \phi(t, x) &= \hat{\phi}_\omega(x) = \hat{a}_\omega^u \phi_\omega^u(x) + \hat{a}_\omega^v \phi_\omega^v(x) + \sum_{l=1,2} \hat{a}_{-\omega,l}^{u\dagger} (\varphi_{-\omega,l}^u)^*, \\ \int \frac{dt}{2\pi} e^{-i\omega t} \phi(t, x) &= \hat{\varphi}_\omega^\dagger(x) = \hat{a}_\omega^{u\dagger} (\varphi_\omega^u(x))^* + \hat{a}_\omega^{v\dagger} (\varphi_\omega^v(x))^* + \sum_{l=1,2} \hat{a}_{-\omega,l}^u \phi_{-\omega,l}^u. \end{aligned} \quad (49)$$

When compared with Eq. (48), the last two terms describe the two new roots. In the first line, a complex conjugate and a subscript  $-\omega$  have been used to characterize the two new modes. This means that the two doublets  $W_{-\omega,l}^u = (\phi_{-\omega,l}^u, \varphi_{-\omega,l}^u)$  have a positive norm and obey Eq. (14) with a frequency  $i\partial_t = -\omega < 0$ .

Finally, it should be noticed that when using the Fourier operators  $\hat{\phi}_\omega(x), \hat{\varphi}_\omega(x)$  of Eq. (49) which contain both annihilation and creation sectors, the field  $\phi$  can still be written as in Eq. (47), as an integral over  $\omega \in [0, \infty]$ . We shall do so in the sequel.

### 3. Inhomogeneous condensates

In metrics which contain a transition from a subsonic to a supersonic flow, the decomposition of  $(\hat{\phi}_\omega, \hat{\varphi}_\omega)$  is modified: because of the scattering on  $v(x)$ , the modes associated with the asymptotic solutions  $e^{ik_\omega x}$  (with  $k_\omega$  a solution of Eq. (36)), that are bounded on one side of the horizon, are generally not bounded on the other side. However, using the linearity of the BdG equations, one can always construct bounded modes as linear combinations of the former modes, requiring that the coefficient of any the growing mode be zero. In the present case, when  $\omega < \omega_{\max}$ , there is only one growing mode in the subsonic asymptotic region. One can then verify that three independent bounded linear combinations can be constructed. Thus  $\hat{\phi}_\omega$ , instead of Eq. (49), should be written:

$$\hat{\phi}_\omega(x) = \hat{a}_\omega^u \phi_\omega^u(x) + \hat{a}_\omega^v \phi_\omega^v(x) + \hat{a}_{-\omega}^{u\dagger} (\varphi_{-\omega}^u(x))^* , \quad (50)$$

and similarly for  $\hat{\varphi}_\omega(x)$ . In this expression,  $\phi_\omega^u$ ,  $\phi_{-\omega}^u$  and  $\varphi_{-\omega}^u$  stand for yet unspecified, normalized bounded modes. The particular cases of the in and out bases shall be defined in the next section.

Instead, for  $\omega > \omega_{\max}$ , there is one growing mode on each side of the horizon and only two independent bounded linear combinations can be constructed, so that nothing changes wrt the homogeneous case and  $\hat{\phi}_\omega$  should still be decomposed as in Eq. (48).

In brief, in the stationary infinite condensates described by Eq. (34), at fixed  $|\omega|$ , the dimensionality of the space of asymptotically bounded solutions of Eq. (17) is three when  $|\omega| < \omega_{\max}$ , and only two when  $|\omega| > \omega_{\max}$ .

## D. Bogoliubov transformation

### 1. Vacuum instability and spontaneous pair production

Since we are dealing with a stationary situation, the energy of the state of  $\phi$  is constant. Hence, one might have thought that no phonons could possibly be spontaneously emitted. This is not the case, because the vacuum is unstable against the production of phonon pairs when two conditions are met. First, negative energy excitations must exist. We saw in the former subsection that it is the case for  $\omega < \omega_{\max}$ , which requires the flow to be supersonic. However, this is not enough, as can be understood by considering a homogeneous condensate

propagating in a frictionless translation faster than sound in the lab frame. One also needs spatial gradients to define unambiguously the unique “preferred” stationary frame, and to couple the so-defined negative energy excitations to positive energy ones, so that each produced pair carries no energy. When these conditions are met, the subset of states having the same energy as the vacuum is highly degenerate.

To see this it is sufficient to write the Hamiltonian operator of the  $\phi$  field, the generator of the time translation in the preferred frame. In stationary inhomogeneous flows which contain a transition from sub- to supersonic motion, the Hamiltonian always has the following structure

$$\begin{aligned}
H = & \int_0^{\omega_{\max}} d\omega \hbar\omega \left( \hat{a}_\omega^{u\dagger} \hat{a}_\omega^u + \hat{a}_\omega^{v\dagger} \hat{a}_\omega^v - \hat{a}_{-\omega}^{u\dagger} \hat{a}_{-\omega}^u \right) \\
& + \int_{\omega_{\max}}^{\infty} d\omega \hbar\omega \left( \hat{a}_\omega^{u\dagger} \hat{a}_\omega^u + \hat{a}_\omega^{v\dagger} \hat{a}_\omega^v \right). \tag{51}
\end{aligned}$$

From this expression three conclusions can be drawn. First the phonons with  $\omega > \omega_{\max}$  cannot participate in the pair production since no partner with the corresponding negative frequency exists. Second, both  $u$  and  $v$  positive frequency modes participate in the vacuum instability. Which of the two channels is most contributing depends on the intensity of the coupling with the negative frequency excitations. Third, the diagonalization of  $H$  in the sector  $0 < \omega < \omega_{\max}$  is ambiguous because by a unitary ( $\omega$ -diagonal) Bogoliubov transformation, the above quadratic form is left unchanged.

Therefore, one needs an additional physical criterion to remove this ambiguity. In the general (time dependent) case no such criterion exists, and the notion of *phonon* is inherently ambiguous [17, 22]. However, in the present case of stationary asymptotically homogeneous condensates, there is no ambiguity. In fact the existence of the two asymptotic regions allow to define without ambiguity two complete sets of modes. The first set of modes (the “in” modes) characterizes the initial phonons propagating towards the sonic horizon. The second set, the “out” modes, is needed to characterize the asymptotic particle content (i.e., the spectral properties) of the scattered field configurations. Having the two sets we can compute how they are related and how this governs the decay of the vacuum.

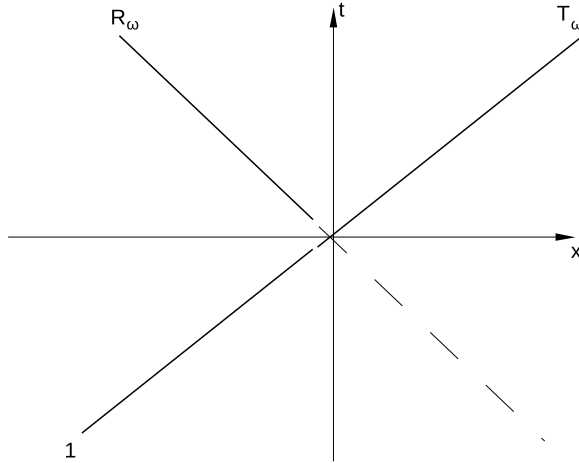


Figure 4: Space-time representation of a wave-packet made out of modes  $\phi_\omega^{u,in}$ , for  $\omega > \omega_{\max}$ .

## 2. Space-time structure of in and out wave-packets

The procedure to identify the in and out modes is standard [20]. One should construct “broad wave packets”, i.e., superpositions of modes at fixed  $\omega$ , so as to extract the asymptotic temporal behavior by looking at the stationary phase condition  $\partial_\omega S = 0$ . This equation is equivalent to Hamilton’s equation since the mode phase  $S$  coincides with the Hamilton-Jacobi action in the asymptotic regions. Having obtained the asymptotic temporal behavior, there is no ambiguity/difficulty in identifying the modes (in fact the doublets  $W_{\omega,a} = (\phi_{\omega,a}, \varphi_{\omega,a})$ ) that are associated with each initial (and final) one-phonon state.

It is useful to visualize these modes. Let us first describe the in mode  $\phi_\omega^{u,in}$ , i.e., the particular solution of Eq. (16) which contains in the past only a right moving packet of asymptotic wave vector  $k^u(\omega)$ .

We shall do it twice, both for  $\omega > \omega_{\max}$ , where there is only some elastic scattering (see Fig. 4), and for  $\omega < \omega_{\max}$ , in the presence of pair creation (see Fig. 5). In both cases, initially, one only has the incoming branch which possesses a unit norm. At late time, depending on whether  $\omega > \omega_{\max}$  or not, one has two or three branches. When  $\omega > \omega_{\max}$ , one has a transmitted  $u$ -mode with amplitude  $T_\omega$ , and a reflected mode with amplitude  $R_\omega$ . Instead for  $\omega < \omega_{\max}$ , in addition to these modes there is the negative frequency mode described by  $(\varphi_{-\omega}^{u,out})^*$  and with an amplitude we shall call  $\beta_{-\omega}$ . The description of the other in and out modes is obtained without difficulty.

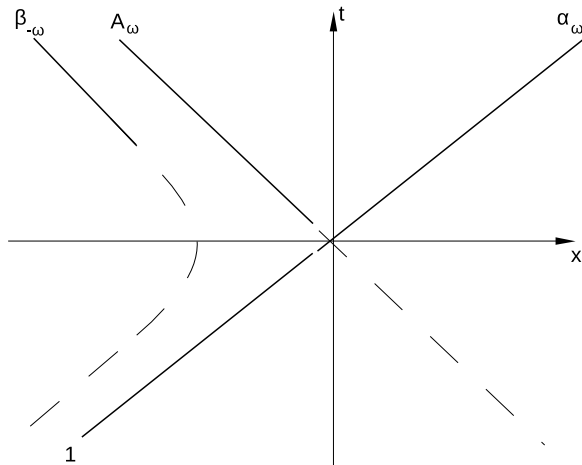


Figure 5: Same as Fig. 4 for  $\omega < \omega_{\max}$ , when pair production occurs.

### 3. Bogoliubov transformation

From Eq. (51) one sees that for  $\omega > \omega_{\max}$  one has only two modes with positive frequency/energy. Because the background in which they propagate is not translation invariant, there will be some scattering. Therefore, in and out  $\phi$  modes will be related by

$$\begin{aligned}\phi_\omega^{u,in} &= T_\omega \phi_\omega^{u,out} + R_\omega \phi_\omega^{v,out}, \\ \phi_\omega^{v,in} &= -R_\omega^* \phi_\omega^{u,out} + T_\omega^* \phi_\omega^{v,out}.\end{aligned}\tag{52}$$

The other modes, the  $\varphi_\omega^{u/v,in/out}$ , are related among themselves by the same relations. Since there is no mixing of  $\phi_\omega$  with  $\varphi_\omega^*$ , the conservation of the norm trivially implies  $|T_\omega|^2 + |R_\omega|^2 = 1$ . One is thus dealing with an elastic scattering between  $u$  and  $v$  modes, and  $T_\omega$ ,  $R_\omega$  are the transmitted and reflected amplitudes, respectively. This is a “trivial” transformation in the sense that there is no spontaneous pair production. The vacuum of these high frequency modes is thus stable.

It should be pointed out that this elastic scattering is also found, for all modes, when the flow remains everywhere subsonic. From this it is tempting to conclude that the high frequency modes with  $\omega > \omega_{\max}$  do not see/experience the presence of the horizon. This simple reasoning is correct and confirmed by looking at the trajectories followed by wavepackets centered around some  $\omega > \omega_{\max}$ . The trajectories are indeed very similar to those obtained when the flow remains subsonic.

The situation is radically different for  $\omega < \omega_{\max}$ . In this case the transformation is non trivial, and three equations are needed to characterize the relationships in the three mode sector

$$\begin{aligned}\phi_{\omega}^{u,in} &= \alpha_{\omega} \phi_{\omega}^{u,out} + \beta_{-\omega} (\varphi_{-\omega}^{u,out})^* + \tilde{A}_{\omega} \phi_{\omega}^{v,out}, \\ \phi_{\omega}^{v,in} &= \alpha_{\omega}^v \phi_{\omega}^{v,out} + B_{\omega} (\varphi_{-\omega}^{u,out})^* + A_{\omega} \phi_{\omega}^{u,out}, \\ \phi_{-\omega}^{u,in} &= \alpha_{-\omega} \phi_{-\omega}^{u,out} + \beta_{\omega} (\varphi_{\omega}^{u,out})^* + \tilde{B}_{\omega} (\varphi_{\omega}^{v,out})^*.\end{aligned}\tag{53}$$

The coefficients are given by the overlap of the corresponding (normalized) in and out doublets, e.g.

$$\beta_{-\omega} = -(\bar{W}_{-\omega}^{u,out}, W_{\omega}^{u,in}).\tag{54}$$

The normalization of the coefficients then immediately follows, e.g. the first equation (together with the corresponding one for  $\varphi_{\omega}^{u,in}$ ) gives

$$|\alpha_{\omega}|^2 + |\tilde{A}_{\omega}|^2 - |\beta_{-\omega}|^2 = 1.\tag{55}$$

In this expression, the minus sign comes from complex conjugated (negative norm) doublets,  $\bar{W} = (\varphi^*, \phi^*)$ , see Eq. (44).

It should be noticed that the above enlarged Bogoliubov transformation governs the general case. It applies indeed to any stationary situation when there is one type of negative frequency modes (here the  $u$ -modes). It should also be noticed that in situations with more than one sonic horizon, there could be several types of modes with negative frequency. In this case, the Bogoliubov transformation will be more complicated than Eq. (53) [23, 24].

### E. Observables: fluxes, density fluctuations, and correlations

Most of the work dedicated to the Hawking effect concentrates on the particle content, or the energy content, of the outgoing flux [17, 22]. These two observables are related to  $|\beta_{\omega}|^2$ , the norm square of the  $\beta_{\omega}$  coefficient in Eq. (53). However, it was also noticed that there are specific correlations between the outgoing particles and their partners with negative frequency  $\omega$ . Unlike the energy flux, these correlations originate from interfering terms (i.e., nondiagonal in the occupation number), they are weighted by  $\alpha_{\omega}\beta_{\omega}^*$ , and they result from the fact that particles are produced from vacuum in pairs which carry zero energy, in virtue of the stationarity of the background.

In the case of gravitational black holes, these correlations are hidden for the external observers because the partners propagate on the other side of the horizon, in the trapped region [20]. Nevertheless these correlations have well-defined properties [25]. Moreover, they extend to the past of the black hole formation and can be revealed by sending quanta to stimulate the emission process [26, 27, 28].

With the advent of acoustic black holes, the situation completely changes because one can have access to both regions. Therefore, one can probe the correlations between the phonons and their partners. In this respect, acoustic black holes are similar to what is found in the homogeneous time-dependent BEC configurations studied in [15, 16, 29, 30], and inflationary cosmology. In that case, the primordial fluctuations, seeds of the galaxy clusters and of the temperature anisotropies in the Cosmic Microwave Background, also result from pair creation [31], and moreover, their correlations possess a well-defined space-time structure [32] which affects today's observables because both members are within our Hubble patch.

Let us first study the occupation numbers, which is more conventional and simpler, and then study the local density fluctuations and nonlocal density correlations.

### 1. Occupation numbers in the initial vacuum

Let us first consider the in vacuum  $|0_{in}\rangle$ , i.e., the state annihilated by the destruction operators  $\hat{a}_\omega^{u,in}$ ,  $\hat{a}_\omega^{v,in}$  and  $\hat{a}_{-\omega}^{u,in}$ , defined by the in modes through Eq. (45). For gravitational black holes, this is the physically relevant state (for outgoing  $u$ -configurations) after a few  $e$ -folding times  $\Delta t = 1/\kappa$ . In fact, because of the exponential redshift effect associated with the near horizon propagation, see Eq. (32), the transient effects due to infalling quanta are exponentially rapidly washed out. Therefore, the choice of the initial distribution of quanta does not affect the stationary properties of the outgoing flux. This is no longer necessarily true for acoustic black holes, because the dispersion limits the number of  $e$ -folding times during which Eq. (32) applies [13, 33]. Thus, one should analyze each case with care to see if the vacuum state is a reliable approximation or not.

Assuming this is the case, the mean occupation numbers of the three types of phonons

are

$$\begin{aligned}
\bar{n}_\omega^{\text{vac}} &= \langle 0_{in} | \hat{a}_\omega^{u, out \dagger} \hat{a}_\omega^{u, out} | 0_{in} \rangle = |\beta_\omega|^2, \\
\bar{n}_\omega^{\text{vac}, v} &= \langle 0_{in} | \hat{a}_\omega^{v, out \dagger} \hat{a}_\omega^{v, out} | 0_{in} \rangle = |\tilde{B}_\omega|^2, \\
\bar{n}_{-\omega}^{\text{vac}} &= \langle 0_{in} | \hat{a}_{-\omega}^{u, out \dagger} \hat{a}_{-\omega}^{u, out} | 0_{in} \rangle = |\beta_{-\omega}|^2 + |B_\omega|^2 = \bar{n}_\omega^{\text{vac}} + \bar{n}_\omega^{\text{vac}, v}.
\end{aligned} \tag{56}$$

These expressions follow when using Eq. (53) and Eq. (45) to express the out operators in terms of in ones.

When compared with the simplified case where  $u$  and  $v$  modes are strictly decoupled [20] two novel effects are found. First,  $v$ -quanta are also produced (to the left of the horizon, in the “inside” region when using the gravitational analogy) and their mean occupation number is  $\bar{n}_\omega^{\text{vac}, v}$ . Secondly, the mean number of  $u$  phonons, emitted to the right  $\bar{n}_\omega^{\text{vac}}$ , or to the left  $\bar{n}_{-\omega}^{\text{vac}}$ , differ:  $\bar{n}_{-\omega}^{\text{vac}} > \bar{n}_\omega^{\text{vac}}$ . In fact,  $\bar{n}_{-\omega}^{\text{vac}} = \bar{n}_\omega^{\text{vac}} + \bar{n}_\omega^{\text{vac}, v}$  tells us that there are now two different channels to produce asymptotic phonons of frequency  $-\omega$ : either through the usual channel where the partner is a Hawking  $u$ -quantum reaching  $x = \infty$ , or through the new channel where the partner is a  $v$ -quantum. When this new channel is negligible, i.e., when  $|\tilde{B}_\omega|^2 \ll |\beta_\omega|^2$ , one recovers the simplified situation where  $\bar{n}_{-\omega}^{\text{vac}} = \bar{n}_\omega^{\text{vac}}$ .

## 2. Occupation numbers from an initial thermal state

In realistic situations, there will always be some residual temperature. In a BEC, the order of magnitude of this temperature is related to the inverse of the healing length  $\xi$ . Moreover, the characteristic wavelength of the condensate inhomogeneity  $\sim c/\kappa$  will always be larger than  $\xi$ . Therefore, since the Hawking temperature is  $k_B T_H = \hbar\kappa/2\pi$ , one expects that the initial distribution of phonons could completely hide the signal caused by the Hawking effect.

For simplicity, to characterize the initial state, we assume that the three distributions have the same temperature. Using  $\Omega^{in}$ , the initial value of the comoving frequency, the three initial occupation numbers  $\bar{n}_\omega^{in}, \bar{n}_\omega^{in, v}, \bar{n}_{-\omega}^{in}$  are

$$\bar{n}_\omega^{in, a} = \left( e^{\beta_T \Omega^{in, a}(\omega)} - 1 \right)^{-1}, \tag{57}$$

where  $\beta_T$  is related to the (initial) temperature by  $k_B T_{in} = \hbar/\beta_T$ . This choice means that, before the scattering in the near horizon region, the temperature measured in the frame comoving with the fluid is the same for all modes.

However, because of the scattering, modes sharing the same constant frequency  $\omega$  mix. Hence we must use  $\omega$  to characterize the initial distributions. For each type of modes, we thus need to express  $\Omega^{in}$  in terms of  $\omega$ . This explains the presence of the index  $a$  in the comoving frequency in the above equation. Using Eq. (36), the values corresponding to the three in modes of Eq. (53) are

$$\begin{aligned}\Omega^{in,u}(\omega) &= \omega - v_- k^u(\omega), \\ \Omega^{in,v}(\omega) &= \omega - v_+ k^v(\omega), \\ \Omega^{in,u}(-\omega) &= -\omega - v_- k^u(-\omega),\end{aligned}\tag{58}$$

where the three roots  $k^u(\omega) > 0, k^v(\omega) < 0, k^u(-\omega) > 0$ , are clearly seen in Fig. 1.

Given the initial occupation numbers, Eq. (53) fixes the final occupation numbers to be

$$\begin{aligned}\bar{n}_\omega^{\text{fin}} &= \bar{n}_\omega^{\text{in}} + |A_\omega|^2 (\bar{n}_\omega^{\text{in},v} - \bar{n}_\omega^{\text{in}}) + |\beta_\omega|^2 (1 + \bar{n}_{-\omega}^{\text{in}} + \bar{n}_\omega^{\text{in}}), \\ \bar{n}_\omega^{\text{fin},v} &= \bar{n}_\omega^{\text{in},v} + |\tilde{A}_\omega|^2 (\bar{n}_\omega^{\text{in}} - \bar{n}_\omega^{\text{in},v}) + |\tilde{B}_\omega|^2 (1 + \bar{n}_{-\omega}^{\text{in}} + \bar{n}_\omega^{\text{in},v}), \\ \bar{n}_{-\omega}^{\text{fin}} &= \bar{n}_{-\omega}^{\text{in}} + |\beta_{-\omega}|^2 (1 + \bar{n}_{-\omega}^{\text{in}} + \bar{n}_\omega^{\text{in}}) + |B_\omega|^2 (1 + \bar{n}_{-\omega}^{\text{in}} + \bar{n}_\omega^{\text{in},v}).\end{aligned}\tag{59}$$

The interpretation of these equations is clear. The first term is the corresponding initial occupation number. Then for the first two lines, the second term is due to the elastic scattering between  $u$  and  $v$  modes which adds (or subtract) particles according to the strength of the scattering, whereas the last term is due to the induced emission which involves both the partner's initial occupation number  $\bar{n}_{-\omega}^{\text{in}}$  and that of the species itself. In the third line instead, one has two induced emission terms because there are two ‘‘pair creation’’ channels and no ‘‘elastic’’ channel.

### 3. Discussions: how to get rid of thermal noises?

From the first line of Eq. (59), one can easily imagine that the Hawking radiation (HR), that is, the spontaneous creation of pairs weighted by  $|\beta_\omega|^2$ , given in the first line of Eq. (56), might be hidden by the presence of initial distributions. See also [12] for a discussion of the consequences of three-phonon interactions.

There is yet another difficulty which can complicate the detection of HR, namely the possibility to distinguish right- from left-moving phonons. In the case one can, detecting HR requires that  $|\beta_\omega|^2$  be larger than, or at least of the same order as, both  $\bar{n}_\omega^{\text{in}}$  and  $|A_\omega|^2 \bar{n}_\omega^{\text{in},v}$ .

The first condition could be satisfied because the initial distribution of  $u$  modes can be significantly redshifted. By this we mean that one can have  $\Omega^{in,u}(\pm\omega) \gg \omega$  and thus possibly  $\Omega^{in,u}(\pm\omega)/T_{in} \gg \omega/T_H$ , although *a priori*  $T_{in} \gg T_H$ . The second condition might be more problematic to fulfill because the  $v$  modes are hardly redshifted. Hence only if  $|A_\omega|^2 \bar{n}_\omega^{in,v} \lesssim |\beta_\omega|^2$  could there be a chance to detect an excess in the outgoing  $u$  spectrum that could be attributed to the pair creation process. This inequality could also be satisfied because, as we shall see, in certain cases the  $u-v$  mixing is very small. Therefore, when one is able to distinguish left- from right-moving phonons, it could be possible to detect Hawking radiation, even when the initial temperature is larger than Hawking temperature. In Secs. IV C and IV C 1, we study numerically realistic situations and confirm this possibility.

In the case one cannot distinguish left- from right-moving phonons, the situation is much worse, because the dominant noise term would be  $\bar{n}_\omega^{in,v}$  since  $v$ -modes are hardly redshifted. Then, as one might have expected, an initial temperature larger than Hawking temperature does indeed hide the presence of Hawking Radiation.

Before proceeding to the numerical analysis, we first study density fluctuations and non-local density correlations for the following reasons. First, occupation numbers are not as such observable quantities. What could be probed are density fluctuations. Second, nonlocal density correlations are also observable (at least in principle), and more importantly, instead of being smeared by the thermal distributions, they are amplified by them, as we shall see.

The reader interested in the spectral properties of the occupation numbers can read Sec. IV first and go back afterwards to the next section.

## F. Density fluctuations

Given that  $\phi$  is a complex field, there are several ways to characterize the fluctuations in BEC: either through the density-density correlation function which is governed by  $\text{Re } \phi$ , see Eq. (22), or through the phase correlations governed by  $\text{Im } \phi$ , or even through the crossed phase-density correlations. In what follows we only discuss the density-density correlations as the extension to the two other types is easily made.

To simplify the forthcoming expressions we introduce the field operator  $\chi = 2\text{Re } \phi$ . In stationary cases, it can be decomposed as in Eq. (47), and in terms of the same destruction and creation operators as those of Eq. (50). The only change is that the c-number wave

functions  $\phi_\omega^a, \varphi_\omega^a$  are all replaced by  $\chi_\omega^a$  given by

$$\chi_\omega^a(x) = \phi_\omega^a(x) + \varphi_\omega^a(x). \quad (60)$$

Since this correspondance applies to both the in and out set of modes, and since both  $\phi_\omega^a$  and  $\varphi_\omega^a$  obey the Bogoliubov transformation of Eq. (53), the three initial  $\chi_\omega^{in,a}$  are related to the three final  $\chi_\omega^{out,a}$  by Eq. (53). Therefore, even though  $\chi$  is not a canonical field, as it does not obey canonical commutators, it can be treated as a genuine quantum field when computing its correlation functions.

The statistical properties of the density fluctuations encoded in a given state are characterized by the correlator

$$\begin{aligned} G^{in}(t, x; t', x') &= \text{Tr}[\hat{\rho}^{in} \chi(t, x) \chi(t', x')], \\ &= \int_{-\infty}^{\infty} d\omega e^{-i\omega(t-t')} G_\omega^{in}(x, x'), \end{aligned} \quad (61)$$

where  $\hat{\rho}^{in}$  is the initial density matrix, since we work in the Heisenberg representation. In the second line we passed to a Fourier transform since we have assumed that both the condensate and the state are stationary (in the ‘‘preferred’’ frame).

When the initial state  $\hat{\rho}^{in}$  is incoherent, using the in operators (and the in modes) to express  $\chi$ , only three terms having the same structure are obtained

$$\begin{aligned} G_\omega^{in}(x, x') &= (\bar{n}_\omega^{in} + 1/2) \chi_\omega^{in,u}(x) (\chi_\omega^{in,u}(x'))^* \\ &+ (\bar{n}_\omega^{in,v} + 1/2) \chi_\omega^{in,v}(x) (\chi_\omega^{in,v}(x'))^* \\ &+ (\bar{n}_{-\omega}^{in} + 1/2) (\chi_{-\omega}^{in,u}(x))^* \chi_{-\omega}^{in,v}(x'). \end{aligned} \quad (62)$$

This expression is valid for  $\omega > 0$ , for  $\omega < 0$ , one has  $G_{-\omega}^{in}(x, x') = (G_\omega^{in}(x, x'))^*$  since  $G^{in}(t, x; t', x')$  is real. In the above equation, the initial occupation numbers are given by

$$n_\omega^{in,i} \times \delta^{ij} = \text{Tr}[\hat{\rho}^{in} a_\omega^{in,i\dagger} a_\omega^{in,j}]. \quad (63)$$

Due to the incoherence of  $\hat{\rho}^{in}$ , only the diagonal terms remain. Additional terms would be obtained if the state  $\hat{\rho}^{in}$  contained correlations among the initial configurations. In what follows we assume it does not.

Because of the scattering of the in modes  $\chi_\omega^{in}$  near the sonic horizon,  $G_\omega^{in}(x, x')$  has a rather complicated structure (as can be seen by decomposing the in modes into out ones).

As we shall see  $G_\omega^{\text{in}}(x, x')$  encodes two types of observables. To show this, is appropriate to consider  $G_\omega^{\text{in}}(x, x')$  in two separate cases. First, we shall compute  $G^{\text{in}}$  in the coincidence point limit,  $x = x'$ , far away from the sonic horizon so that the scattering is completed, and both on the left and right regions. In these cases it depends on the occupation numbers of Eq. (59), and governs the power spectrum of the density fluctuations. Secondly, we shall compute it for very different values of  $x$  and  $x'$ , again far away from the horizon. In this second case, it governs the long distance correlations and depends on nondiagonal correlators such as  $\text{Tr}[\hat{\rho}^{\text{in}} a_\omega^{\text{out}, i} a_\omega^{\text{out}, j}]$  with  $i \neq j$ .

### G. Coincidence point limit and density fluctuations.

Far from the horizon, i.e., when  $|x| \gg Dc_0/\kappa$ , one should express the in modes in terms of their asymptotic plane wave content  $\sim e^{ik_\omega^a x}$ . To ease the reading, we shall call these asymptotic contributions by the corresponding wave,  $\chi_\omega^{\text{in}, a}$  or  $\chi_\omega^{\text{out}, a}$ , for which the amplitude of this contribution is unity, and, to avoid any misinterpretation, we shall add an upper index “as” to make clear that only that unit, plane wave contribution should be kept. In terms of these, using Eq. (59), in the asymptotic right region, one gets

$$G_\omega^{\text{in}}(x, x) \rightarrow (\bar{n}_\omega^{\text{fin}, u} + 1/2) \times |\chi_\omega^{\text{out}, u, \text{as}}|^2 + (\bar{n}_\omega^{\text{in}, v} + 1/2) \times |\chi_\omega^{\text{in}, v, \text{as}}|^2, \quad (64)$$

whereas, on the left, the “power” is asymptotically equal to

$$\begin{aligned} G_\omega^{\text{in}}(x, x) \rightarrow & (\bar{n}_\omega^{\text{fin}, v} + 1/2) \times |\chi_\omega^{\text{out}, v, \text{as}}|^2 + (\bar{n}_{-\omega}^{\text{fin}, u} + 1/2) \times |\chi_{-\omega}^{\text{out}, u, \text{as}}|^2 \\ & + (\bar{n}_\omega^{\text{in}, u} + 1/2) \times |\chi_\omega^{\text{in}, u, \text{as}}|^2 + (\bar{n}_{-\omega}^{\text{in}, u} + 1/2) \times |\chi_{-\omega}^{\text{in}, u, \text{as}}|^2. \end{aligned} \quad (65)$$

Since the point  $x = x'$  lives in an asymptotic region where the condensate is homogeneous, the norm of the asymptotic modes  $\chi_\omega^{\text{as}}$  is  $x$  independent. Notice also that we have discarded all oscillatory terms, such as  $\chi_\omega^{\text{out}, u, \text{as}} (\chi_\omega^{\text{in}, v, \text{as}})^* \sim e^{i(k_\omega^u - k_\omega^v)x}$ , because they rapidly oscillate as  $x \rightarrow \infty$ , and thus drop out when averaging a bit over  $\omega$ .

The interpretation of the above equations is clear. When working in the state  $\hat{\rho}^{\text{in}}$ , the two asymptotic values of the correlator are the sum of the contributions of the waves that have been scattered, governed by the final occupation numbers,

$$n_\omega^{\text{fin}, i} = \text{Tr}[\hat{\rho}^{\text{in}} a_\omega^{\text{out}, i \dagger} a_\omega^{\text{out}, i}], \quad (66)$$

and of the waves which have not propagated through the horizon region, and whose occupation numbers are the initial ones given in Eq. (63). From Eq. (64) one clearly sees that the second term (the  $v$  contribution) will hide the Hawking radiation whenever  $\bar{n}^{\text{in},v}$  is much larger than  $\bar{n}^{\text{fin},u}$ , which is the case in realistic situations, as we shall see in Sec. IV C 2.

It is therefore also of interest to compute

$$\begin{aligned}\mathcal{F}(t, x; t', x') &= \frac{i\hbar}{2\rho_0}(\partial_{x'} - \partial_x)\text{Tr} [\hat{\rho}^{\text{in}} \Psi^\dagger(t', x') \Psi(t, x)] \\ &= \int_{-\infty}^{\infty} d\omega e^{-i\omega(t-t')} \mathcal{F}_\omega(x, x').\end{aligned}\tag{67}$$

In the coincidence point limit  $(t, x) = (t', x')$ ,  $\rho_0\mathcal{F}/m$  is the atom flux at  $(t, x)$ . Using Eq. (13), one finds that the atom flux in the asymptotic right region is the sum of the background flux  $\rho_0v = \rho_0\hbar k_0/m$  and of a contribution fixed by the function  $\mathcal{F}_\omega$  given by:

$$\mathcal{F}_\omega(x, x) = (\bar{n}_\omega^{\text{fin}} + 1/2) \times \hbar(k_\omega^{u,\text{out}} + k_0) |\phi_\omega^{u,\text{out},\text{as}}(x)|^2 + (\bar{n}_\omega^{\text{in},v} + 1/2) \times \hbar(k_\omega^{v,\text{in}} + k_0) |\phi_\omega^{v,\text{in},\text{as}}(x)|^2,\tag{68}$$

for  $\omega > 0$ , and by the same expression with opposite signs and  $\phi$  replaced by  $\varphi$  for  $\omega < 0$ . As in the case of the density fluctuations, the term arising from the initial distribution of  $v$ -phonons dominates largely. However, since  $k_\omega^{v,\text{in}} < 0$ ,  $\mathcal{F}_\omega$  contains a contribution related to the *difference* of the terms appearing in  $G_\omega^{\text{in}}(x, x)$ , up to  $k$ -dependent factors (different for each term). Thus, if one has access to both the atom flux and the density fluctuations in the right asymptotic region, there is a greater hope to have access to  $\bar{n}_\omega^{\text{fin}}$ .

Nevertheless, the fact that both the atom flux and the density fluctuations are *a priori* largely dominated by the distribution of initial quanta reinforces the interest to consider observables that are not erased by them.

## H. Long distance correlations.

When looking at equal time and long distance correlations

$$|x - x'| \gg Dc_0/\kappa > \xi_0,\tag{69}$$

$G_\omega^{\text{in}}(x, x')$  displays a completely different structure. When considering the correlations far away from the horizon, one can again use the asymptotic modes  $\chi^{\text{as}}$ .

### 1. Late time entanglement

Looking first at correlations across the horizon,  $x > 0$ ,  $x' < 0$ , one gets eight terms, since one has two asymptotic modes on the right, and four on the left, see Eq. (49). However, many of them vanish for the following reasons. First, when the initial state  $\hat{\rho}^{\text{in}}$  is incoherent, no (long distance) correlations among in modes exist, as already discussed. Secondly, all correlations between in and out  $\chi^{\text{as}}$  modes will destructively interfere to zero upon integrating over  $\omega$ , as their phase variation involve the large Hamilton-Jacobi time needed for a mode to go from  $x$  to  $x'$ . Therefore, only correlations among asymptotic out modes could possibly contribute. These will contribute because the out phonons have been entangled by the interaction (here the scattering by the spatial gradients), as in a measurement process.

These late time correlations are thus governed by the only two terms involving out modes, and  $G_{\omega}^{\text{in}}(x, x')$  has the form:

$$G_{\omega}^{\text{in}}(x, x') = \chi_{\omega}^{\text{out}, u, \text{as}}(x) \times (\mathcal{A}_{\omega} (\chi_{\omega}^{\text{out}, v, \text{as}}(x'))^* + \mathcal{B}_{\omega} \chi_{-\omega}^{\text{out}, u, \text{as}}(x')). \quad (70)$$

Had we looked at equal time correlations with both  $x$  and  $x'$  on the right, no long distance correlations could have been found because there is only one asymptotic out mode in the subsonic region, namely  $\chi_{\omega}^{\text{out}, u, \text{as}}$ . On the contrary, when both  $x$  and  $x'$  are negative, in the supersonic region on the left of the horizon, two asymptotic modes exist:  $\chi_{\omega}^{\text{out}, v, \text{as}}$  and  $\chi_{-\omega}^{\text{out}, u, \text{as}}$ . Since they mix by the Bogoliubov transformation Eq. (53) one expects them to be entangled. This is indeed the case and this shows up through

$$G_{\omega}^{\text{in}}(x, x') = \mathcal{C}_{\omega} \chi_{\omega}^{\text{out}, v, \text{as}}(x) \chi_{-\omega}^{\text{out}, u, \text{as}}(x'). \quad (71)$$

Straightforward calculation gives the coefficients  $\mathcal{A}_{\omega}$ ,  $\mathcal{B}_{\omega}$  and  $\mathcal{C}_{\omega}$  :

$$\begin{aligned} \mathcal{A}_{\omega} &= (\bar{n}_{\omega}^{\text{in}} + 1/2) \alpha_{\omega} \tilde{A}_{\omega}^* + (\bar{n}_{\omega}^{\text{in}, v} + 1/2) A_{\omega} \alpha_{\omega}^{v*} + (\bar{n}_{-\omega}^{\text{in}} + 1/2) \beta_{\omega}^* \tilde{B}_{\omega}, \\ \mathcal{B}_{\omega} &= (\bar{n}_{\omega}^{\text{in}} + 1/2) \alpha_{\omega} \beta_{-\omega}^* + (\bar{n}_{\omega}^{\text{in}, v} + 1/2) A_{\omega} B_{\omega}^* + (\bar{n}_{-\omega}^{\text{in}} + 1/2) \beta_{\omega}^* \alpha_{-\omega}, \\ \mathcal{C}_{\omega} &= (\bar{n}_{\omega}^{\text{in}} + 1/2) \tilde{A}_{\omega} \tilde{\beta}_{-\omega}^* + (\bar{n}_{\omega}^{\text{in}, v} + 1/2) \alpha_{\omega}^v B_{\omega}^* + (\bar{n}_{-\omega}^{\text{in}} + 1/2) \tilde{B}_{\omega}^* \alpha_{-\omega}. \end{aligned} \quad (72)$$

Using the orthogonality of the out modes, one can rewrite these expressions in a way which clearly separates the vacuum correlations from the additional ones in nonvacuum states

$$\begin{aligned} \mathcal{A}_{\omega} &= \bar{n}_{\omega}^{\text{in}} \alpha_{\omega} \tilde{A}_{\omega}^* + \bar{n}_{\omega}^{\text{in}, v} A_{\omega} \alpha_{\omega}^{v*} + (\bar{n}_{-\omega}^{\text{in}} + 1) \beta_{\omega}^* \tilde{B}_{\omega}, \\ \mathcal{B}_{\omega} &= \bar{n}_{\omega}^{\text{in}} \alpha_{\omega} \beta_{-\omega}^* + \bar{n}_{\omega}^{\text{in}, v} A_{\omega} B_{\omega}^* + (\bar{n}_{-\omega}^{\text{in}} + 1) \beta_{\omega}^* \alpha_{-\omega}, \\ \mathcal{C}_{\omega} &= \bar{n}_{\omega}^{\text{in}} \tilde{A}_{\omega} \tilde{\beta}_{-\omega}^* + \bar{n}_{\omega}^{\text{in}, v} \alpha_{\omega}^v B_{\omega}^* + (\bar{n}_{-\omega}^{\text{in}} + 1) \tilde{B}_{\omega}^* \alpha_{-\omega}. \end{aligned} \quad (73)$$

In the vacuum, the residual correlations all involve the negative frequency modes because these enter in both pair creation channels.

At this point, several observations should be made. Firstly, given the  $3 \times 3$  character of the Bogoliubov transformation Eq. (53), it was expected that three types of late time correlations would develop since three different types of couples of out modes can be formed.

Secondly, the above coefficients are given by the following nondiagonal correlators

$$\begin{aligned}\mathcal{A}_\omega &= \text{Tr}[\hat{\rho}^{\text{in}} a_\omega^{\text{out},u} a_\omega^{\text{out},v\dagger}], \\ \mathcal{B}_\omega &= \text{Tr}[\hat{\rho}^{\text{in}} a_\omega^{\text{out},u} a_{-\omega}^{\text{out},u}], \\ \mathcal{C}_\omega &= \text{Tr}[\hat{\rho}^{\text{in}} a_\omega^{\text{out},v} a_{-\omega}^{\text{out},u}].\end{aligned}\tag{74}$$

Unlike the coincidence point limit of  $G_\omega^{\text{in}}(x, x')$  which is governed by diagonal terms, see Eqs. (64, 65), the long distance correlations are governed by interfering terms (nondiagonal in occupation number). This is exactly as in inflationary cosmology [32], and in fact will always be found when the parametric amplification (or the scattering) conserves a quantity, the frequency  $\omega$  here, the spatial wave-vector  $\mathbf{k}$  in homogeneous cosmology. Notice also that the operator in the  $\mathcal{A}_\omega$  coefficient, being a product  $a_\omega^u a_\omega^{v\dagger}$ , will be nonzero even in the absence of pair creation, but only when  $n_\omega^{\text{in}} \neq n_\omega^{\text{in},v}$ . (It would be zero otherwise because of the orthogonality of the scattering matrix of Eq. (52).<sup>1</sup>)

Thirdly, because the initial distributions  $\bar{n}^{\text{in},a}$  only appear in factors multiplying terms already present in the in vacuum, the long distance correlations will not be erased by the presence of initial quanta. In fact an initial temperature will in general amplify the long distance correlations induced by interactions. (We added “in general” because the terms in Eq. (72) have no definite sign. Hence, an increase in the temperature can lower, in some cases, the amplitudes of  $\mathcal{A}_\omega, \mathcal{B}_\omega, \mathcal{C}_\omega$ .) This amplification follows from the incoherent character of the initial state which cannot interfere with the correlators of Eq. (74).

Fourthly, this entanglement has been obtained using the BdG equation (16) which neglects phonon interactions [12]. One might therefore worry that the entanglement is reduced upon taking into account such interactions. We refer to Refs. [34, 35, 36] for an analysis of this point in a cosmological context. In brief, the weakness of the nonlinearities guarantees that the entanglement is hardly reduced.

---

<sup>1</sup> We thank C. Mayoral and A. Fabbri for drawing our attention to this particular point.

## 2. Spatial structure of long distance correlations

At fixed  $\omega$  no spatial structure emerges from Eqs. (70, 71). To get the spatial properties of the correlations encoded in these equations, one needs to take the inverse Fourier transform. Then, as it is the case when considering wave packets, constructive interferences will develop along the characteristics of the mode equation. To ease the reading of the forthcoming expression we found convenient to return to Eq. (61) and to re-introduce  $t$  and  $t'$ .

As usual, the constructive interference condition gives the stationary phase condition  $\partial_\omega S = 0$ . In the present case, using a WKB approximation for the modes  $\chi_\omega^a(x) \sim \exp(i \int^x dy k_\omega^a(y))$ , the three phases of the terms weighted by  $\mathcal{A}_\omega$ ,  $\mathcal{B}_\omega$  and  $\mathcal{C}_\omega$  are respectively

$$\begin{aligned} S_A(t, t', x, x'; \omega) &= -\omega(t - t') + \int_z^x dy k_\omega^u(y) - \int_z^{x'} dy k_\omega^v(y) + \arg(\ln \mathcal{A}_\omega) \\ S_B(t, t', x, x'; \omega) &= -\omega(t - t') + \int_z^x dy k_\omega^u(y) + \int_z^{x'} dy k_{-\omega}^u(y) + \arg(\ln \mathcal{B}_\omega) \\ S_C(t, t', x, x'; \omega) &= -\omega(t - t') + \int_z^x dy k_\omega^v(y) + \int_z^{x'} dy k_{-\omega}^u(y) + \arg(\ln \mathcal{C}_\omega) \end{aligned} \quad (75)$$

where  $z$  is an arbitrary location where the absolute (unobservable) phase of the  $\chi_\omega^a$  is fixed. The stationary phase condition gives

$$(t - t') = \int_z^x dy \partial_\omega k_\omega^u(y) - \int_z^{x'} dy \partial_\omega k_\omega^v(y) + \partial_\omega \arg(\ln \mathcal{A}_\omega), \quad (76)$$

for the first line, and similar equations for the second and third lines. (*A priori* it seems that the choice of  $z$  matters. However this is not the case because  $z$  enters in  $\mathcal{A}_\omega$  in such a way that a change of  $z$  leaves the r.h.s. of the equation unchanged. (This is because the coefficients of Eq. (74) contain the operators  $a^\dagger, a$  which are “contravariant” with respect to a phase change of the corresponding mode.) The physically meaningful phase that comes out of these expressions has the role of fixing the location where the interactions occur. [37])

This result becomes exact in the limit where  $x$  and  $x'$  are taken far away from the scattering zone, and it amounts to put  $z = 0$  and to take  $\mathcal{A}_\omega$  real in Eq. (76), and similarly for the two other equations involving  $\mathcal{B}_\omega$  and  $\mathcal{C}_\omega$ . (There could be some finite phase shift with respect to these WKB estimates, but these do not change with  $x$  and  $x'$ , and hence give subdominant effects in the large  $x$  limit. In this limit, the norm and the phase of the three coefficients play no role the correlation pattern.) In this approximation, when putting  $t = t' = 0$ , the stationary phase condition applied to Eq. (75) gives, for the  $\mathcal{A}_\omega$ ,  $\mathcal{B}_\omega$  and  $\mathcal{C}_\omega$

terms respectively,

$$\begin{aligned}
\Delta t_\omega^{HJ, u}(x) &= \Delta t_\omega^{HJ, v}(x'), \\
\Delta t_\omega^{HJ, u}(x) &= \Delta t_{-\omega}^{HJ, u}(x'), \\
\Delta t_\omega^{HJ, v}(x) &= \Delta t_{-\omega}^{HJ, u}(x'),
\end{aligned} \tag{77}$$

where

$$\Delta t_\omega^{HJ, a}(x) = \int_0^x dy \partial_\omega k_\omega^a(y) \tag{78}$$

is the time it takes the  $a$ -type phonon of frequency  $\omega$  to propagate from  $x = 0$  to  $x$ , in virtue of the Hamilton-Jacobi equation determining the group velocity

$$v_{gr}^a(\omega) = (\partial_\omega k_\omega^a)^{-1}. \tag{79}$$

For each type of correlations, we see that the locus of constructive interference of, say,  $x'$  given  $x$ , is given by the value of  $x'$  reached at the same lapse time it takes the partner to reach  $x$ , both phonons starting their journey near the horizon  $x = 0$ . In the large  $x$  limit, the dominant contribution comes from the uniform motion outside the horizon region. Thus the above three constructive interferences occur at locations  $x, x'$  related by

$$\frac{x}{v_{gr}^a(\omega)} = \frac{x'}{v_{gr}^b(\omega)}. \tag{80}$$

Using Eq. (36), the asymptotic group velocities are, for  $x \rightarrow +\infty$ ,

$$v_{gr}^u(\omega) = \partial_k \Omega_+ + v_+ = c_+^2 k \frac{1 + k^2 \xi_+^2}{\Omega_+(k)} + v_+, \tag{81}$$

for the right movers in the subsonic region, the ‘‘Hawking quanta’’; and, for  $x \rightarrow -\infty$ ,

$$\begin{aligned}
v_{gr}^v(\omega) &= -\partial_k \Omega_- + v_- = -c_-^2 k \frac{1 + k^2 \xi_-^2}{\Omega_-(k)} + v_-, \\
v_{gr}^u(-\omega) &= \partial_k \Omega_- + v_- = c_-^2 k \frac{1 + k^2 \xi_-^2}{\Omega_-(k)} + v_-,
\end{aligned} \tag{82}$$

for the left-moving  $v$  quanta and the  $u$  partners with negative frequency in the supersonic region. When the asymptotic wave number  $k$  obeys  $k \ll \xi_\pm$ , i.e., in the dispersionless regime, these group velocities are independent of  $\omega$  and respectively equal to  $c_+ + v_+$  in Eq. (81), and  $-c_- + v_-$ ,  $c_- + v_-$  for Eq. (82).

These three types of correlations have been (numerically) observed in [11]. They have been also correctly interpreted save for two aspects. First, the  $\mathcal{C}_\omega$  branch has been attributed

to the “partial elastic scattering” of right movers of positive frequency which is not fully correct as can be seen from the third line in Eq. (72). If this explanation applies to the first term, it does not to the last two which only involve Bogoliubov coefficients between the  $v$  mode  $\chi_\omega^v$  and  $\chi_{-\omega}^u$ , the  $u$  mode of negative  $\omega$ . Second, the  $\mathcal{A}_\omega$  is claimed to “originate from thermal effects”. From the first line of Eq. (73) we see that it is indeed amplified by thermal effects, but, because of the third term, it is already present in the vacuum. Being quadratic in frequency mixing coefficients, it was probably too weak to have been observed in the numerical simulations.

Concerning the relative amplitude of the coefficients  $\mathcal{A}_\omega$ ,  $\mathcal{B}_\omega$  and  $\mathcal{C}_\omega$  it should be noticed that, in general, there is no clear ordering. Instead, when the  $u - v$  mixing is weak, the Bogoliubov coefficients  $A_\omega$ ,  $B_\omega$  are much smaller than  $\beta_\omega$  (see Sec. IV B 5) and therefore,  $\mathcal{B}_\omega$  should be the largest. In this regime, one recovers the properties of the  $\mathcal{B}_\omega$  branch relating the  $u$  modes across the horizon that have been known for a while. In the context of gravitational black holes, using relativistic fields, they can be found in [20, 25]. As of acoustic black holes, the fact that these correlations are essentially unaffected when taking into account the dispersive properties of the field was understood in [4] and further analyzed in [13] and [33]. Finally, that they determine the long distance density-density correlations in BECs was stressed in [10].

#### IV. SPECTRAL PROPERTIES: NUMERICAL RESULTS

##### A. Value of the parameters

Let us determine the number of free parameters and their realistic ranges.<sup>2</sup> A typical value for the average sound speed  $c_0$  is

$$c_0 = 0.15 \text{ cm} \cdot \text{s}^{-1}. \quad (83)$$

Assuming that the condensate is made out of  $^{85}\text{Rb}$ , the mass of the atoms is

$$m = 1.5 \times 10^{-25} \text{ kg}. \quad (84)$$

---

<sup>2</sup> We are grateful to Eric Cornell for providing us with realistic experimental values for all parameters.

This yields the healing length,

$$\xi_0 = \frac{\hbar}{\sqrt{2}mc_0} = \frac{\sqrt{2}c_0}{\Lambda} \simeq 3.3 \times 10^{-5} \text{ cm.} \quad (85)$$

The distance over which the variation of the sound speed and flow velocity takes place, that is, the distance separating the asymptotic regions where these speeds are constant, cannot be smaller than a few healing lengths. To reduce the number of free parameters, we assume in this work that it is of the order of  $10\xi_0$  (see however Sec. IV B 2). Then, given our parameterization Eq. (35), we impose that:

$$10\xi_0 = \frac{2c_0D}{\kappa}, \quad (86)$$

which implies that the gradient at the horizon is

$$\kappa = \frac{c_0D}{5\xi_0}. \quad (87)$$

With Eq. (85), this yields a relationship between  $D$  and  $\lambda = \Lambda/\kappa$ :

$$\lambda \simeq \frac{7}{D}. \quad (88)$$

as well as an expression for the Hawking temperature:

$$T_H = \frac{\hbar\kappa}{2\pi k_B} \simeq D \times 1.1 \text{ nK}, \quad (89)$$

where we have used Eq. (87) and the numerical values above. We choose as free parameters  $D$  and  $q$ . Thus Eq. (88) fixes  $\lambda$ .

Fairly large relative variations around the average sound speed  $c_0$  can be achieved experimentally, for instance by means of a Feshbach resonance that modifies the coupling constant  $g$  along the flowing BEC. Hence we shall consider values of  $D$  from 0.1 to 0.7 (higher values are not excluded experimentally, but proved difficult to reach with our code). The corresponding values of  $\lambda$  go from 70 to 10, while the order of magnitude of Hawking temperature is

$$T_H \simeq 0.1 - 0.8 \text{ nK.} \quad (90)$$

In general there will be a variation of both the sound speed and the flow velocity. Which one varies most depends on the experimental conditions. In [11],  $q$  was taken to be zero. Our typical value of  $q$  will be 0.3. In Sec. IV B 4, we shall nevertheless explore the whole range  $0 < q < 1$ .

When the condensate is formed, it has a residual temperature approximately given by the healing temperature:

$$T_{\xi_0} = \frac{\hbar c_0}{\xi_0 k_B} \simeq 30 \text{ nK}. \quad (91)$$

This value is only indicative, and in the following we consider residual temperatures

$$T_{\text{res}} = \tau T_{\xi_0}, \quad (92)$$

with  $\tau$  ranging from 1/3 to 1, so that  $T_{\text{res}}$  goes from 10 nK to 30 nK. Equation (91) together with (85) yields

$$\frac{T_{\text{res}}}{T_H} = \tau \times \sqrt{2\pi} \lambda. \quad (93)$$

If  $\lambda$  is constrained by Eq. (88), this can be rewritten as

$$\frac{T_{\text{res}}}{T_H} \simeq 30 \frac{\tau}{D}. \quad (94)$$

The fact that  $T_{\text{res}}$  is about two orders of magnitude higher than the Hawking temperature will surely complicate measuring the spectral properties of Hawking radiation.

In the following sections, we start by studying these spectral properties assuming the condensate has zero temperature. The analysis of when there is an initial temperature is then performed in Sec. IV C. Our main goal is to understand how the adimensional parameters  $D, \lambda, q$  affect the fluxes. To this end it proves very convenient to work with the rescaled frequency  $\omega/\kappa$  and rescaled energy flux  $f_\omega$  defined below.

## B. Spectral properties of HR at zero temperature

Let us first study the energy flux of positive frequency  $u$  quanta on the right of the horizon, i.e., what corresponds to Hawking radiation. We denote by  $F$  the total energy flux, and we define the energy flux density as:

$$f_\omega = \frac{2\pi}{k_B T_H} \frac{dF}{d\omega} = 2\pi \frac{\omega}{\kappa} |\beta_\omega|^2. \quad (95)$$

The factor  $2\pi/k_B T_H$  is here for convenience, so that  $f_\omega$  be dimensionless and normalized to 1 at  $\omega = 0$  when the occupation number  $n_\omega = |\beta_\omega|^2$  is the standard, Planckian one with temperature  $T_H$ . To characterize the deviations from the standard flux, it is convenient to use the effective temperature  $T_\omega$  defined as

$$n_\omega = \frac{1}{\exp(\hbar\omega/k_B T_\omega) - 1}. \quad (96)$$

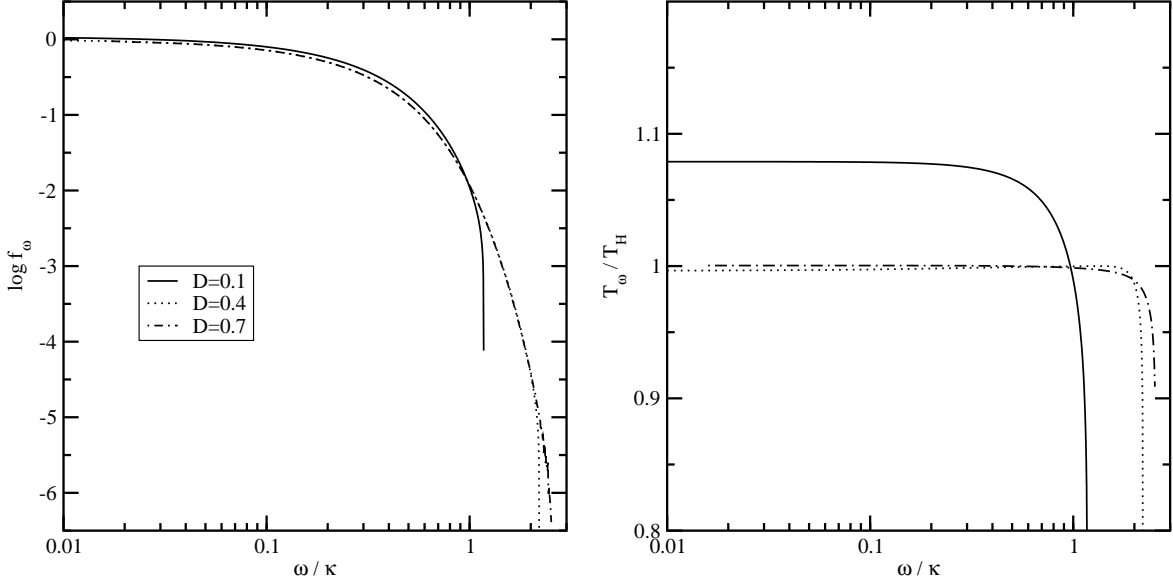


Figure 6: Energy flux density  $f_\omega$  (left plot) and effective temperature  $T_\omega/T_H$  (right plot) versus  $\omega/\kappa$ , for  $(D, \lambda) = (0.1, 70)$ ,  $(0.4, 18)$  and  $(0.7, 10)$ .  $q$  is fixed to 0.3.

### 1. Typical spectra

In Fig. 6 we have represented  $f_\omega$  and  $T_\omega/T_H$  versus  $\omega/\kappa$  for  $D = 0.1, 0.4$  and  $0.7$ . The corresponding  $\lambda$  are fixed by Eq. (88) and are respectively  $\lambda = 70, 18$  and  $10$ . The parameter  $q$  specifying the relative contribution of  $c$  and  $v$  to the gradient at the horizon, see Eq. (35), is fixed to 0.3. The three values of  $\omega_{\max}/\kappa$  are respectively 1.17, 2.2 and 2.54. The energy flux and  $T_\omega$  quickly drop to zero when approaching  $\omega_{\max}$ , as expected. Until short before  $\omega_{\max}$ ,  $T_\omega$  is nearly constant.

Note nevertheless that this constant temperature can differ from  $T_H$ : for  $D = 0.1$ , the asymptotic temperature when  $\omega \rightarrow 0$  is equal to  $T_0 = 1.08T_H$ . For  $D = 0.4$  and  $D = 0.7$ , we found  $T_0 = 0.996T_H$  and  $T_0 = 1.0004T_H$  respectively, so  $T_0$  differs from  $T_H$  only by a fraction of a percent when  $D$  is large enough. Note also that the scale separation condition  $\lambda \gg 1$  is not the relevant criterion to predict the importance of the deviation with respect to the standard spectrum, since  $\lambda$  is much larger for  $D = 0.1$  than for the other two values. Instead, it is the ratio  $\omega_{\max}/\kappa$  that controls the deviation from the standard temperature. This is confirmed in Sec. IV B 3.

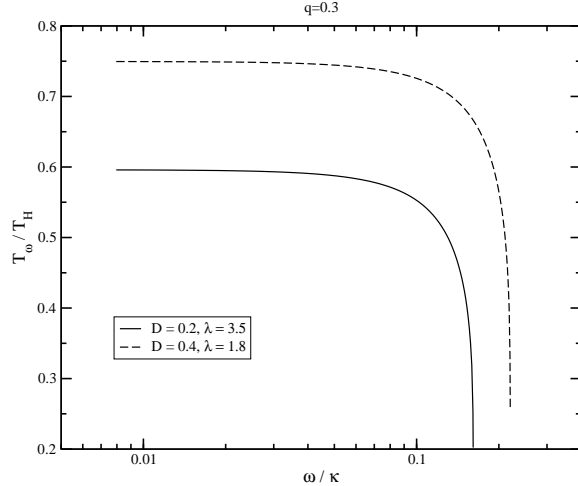


Figure 7: Effective temperature  $T_\omega$  as a function of  $\omega$  for  $q = 0.3$  and  $(D, \lambda) = (0.2, 3.5)$  (solid line) and  $(0.4, 1.8)$  (dashed line).

The thermality of the spectra can be characterized more precisely. To this end we define

$$\Delta_{T_0} = \frac{T_0 - T_{\omega=k_B T_0/\hbar}}{T_0}, \quad (97)$$

that measures the running of the temperature. For the three spectra of Fig. 6, we found  $|\Delta_{T_0}| \simeq 0.1\%$ . This establishes that, to a very good approximation, the energy spectra are Planckian, but truncated very close to  $\omega_{\max}$ .

## 2. Strongly dispersive regimes

In this section, we assume that the variation of  $c+v$  occurs on one healing length instead of ten, as it is assumed in the rest of the text, see the discussion before Eq. (88). This amounts to change the numerical factor in Eq. (88) so that now:

$$\lambda = \frac{0.7}{D}. \quad (98)$$

In Fig. 7, the effective temperature  $T_\omega$  is shown for  $q = 0.3$  and  $(D, \lambda) = (0.2, 3.5)$  and  $(0.4, 1.8)$ . The corresponding values of  $\omega_{\max}/\kappa$  are 0.16 and 0.22, that is, much smaller than in Fig. 6. The shape of the two curves is remarkably similar to what was obtained in the right plot of Fig. 6:  $T_\omega$  is nearly constant as soon as the frequency is less than about  $0.2 \times \omega_{\max}$ , then drops quickly to zero when approaching  $\omega_{\max}$ . However,  $T_0$ , the asymptotic value of  $T_\omega$ , differs significantly from the standard Hawking temperature. It is respectively

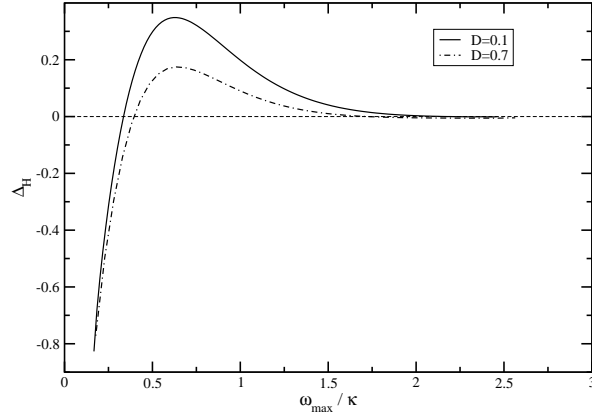


Figure 8:  $\Delta_H$  versus  $\omega_{\max}/\kappa$  for  $D = 0.1$  and  $D = 0.7$ .  $q$  is fixed to 0.3.

equal to  $0.6 T_H$  and  $0.75 T_H$ . The running  $\Delta_{T_0}$  remains small: it is equal to 7% and 5% respectively. From this we conclude that when dispersion is strong, which happens for low values of  $\omega_{\max}/\kappa$ , the spectrum remains a nearly Planckian one, truncated near  $\omega_{\max}$ , but with a temperature that differs from the standard one, and that becomes smaller and smaller as  $\omega_{\max}/\kappa$  decreases.

### 3. $\omega_{\max}/\kappa$ controls the deviation from the standard spectrum

In this section, in order to show that  $\omega_{\max}/\kappa$  is the main quantity that controls the modifications with respect to the standard Planckian spectrum with temperature  $T_H$ , we relax the constraint (88), and allow for arbitrary values of  $\lambda$  for a given  $D$ . We characterize the deviation with respect to the standard result by the relative difference

$$\Delta_H = \left. \frac{f_\omega - f_\omega^H}{f_\omega^H} \right|_{\omega=\omega_H}, \quad (99)$$

as a function of  $\omega_{\max}/\kappa$ , where  $f_\omega^H$  denotes the Planckian energy flux density with temperature  $T_H$ , and  $\omega_H = k_B T_H / \hbar$ .

In Fig. 8, for  $q = 0.3$ , the curves associated with  $D = 0.1$  and  $D = 0.7$  have similar shapes, with a maximum around  $\omega_{\max}/\kappa = 0.6$ , with height 0.35 for  $D = 0.1$  and 0.18 for  $D = 0.7$ . The deviation then decreases and in both cases becomes less than a percent as soon as  $\omega_{\max}/\kappa > 2$ . This confirms what was found (in a different setup) in Ref. [14]. This is not the end of the story however, since as we now show, there can be significant deviations from thermality in a BEC, even when  $\omega_{\max}/\kappa$  is large, depending on the value of the parameter

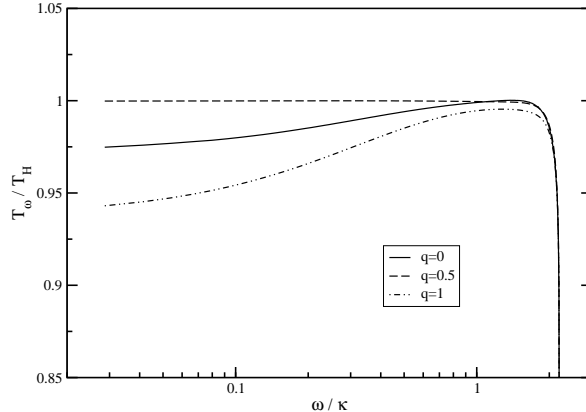


Figure 9: Effective temperature as a function of  $\omega/\kappa$  for  $D = 0.4$  and  $(q, \lambda) = (0, 19.54)$ ,  $(0.5, 17.15)$ ,  $(1, 15.47)$ .  $\omega_{\max}/\kappa$  is the same for all curves, equal to 13.83.

$q$ .

#### 4. Effect of inhomogeneity: deviations from thermality

In the preceding sections, we have fixed  $q = 0.3$ . However, as shown in Fig. 9, the precise mixture of  $c$  and  $v$  used to form the horizon significantly affects the properties of the Hawking flux. In that figure,  $T_\omega/T_H$  is plotted versus  $\omega/\kappa$  for  $D = 0.4$ , and  $q = 0$  (homogeneous BEC where only  $c$  varies),  $q = 0.5$  and  $q = 1$  (only  $v$  varies). For each value of  $q$ ,  $\lambda$  is tuned so that we work at fixed  $\omega_{\max}/\kappa$  to facilitate the comparison. For  $q = 0$  and  $q = 1$ , the effective temperature varies significantly and the radiation is thus not thermal. For  $q = 0.5$ , as in the previous plot with  $q = 0.3$ , the radiation is (almost) thermal. We have verified that the same results hold with other values of  $D$  and  $\lambda$ , with the same particular role of  $q = 0.5$ .

The strong effect of  $q$  on the Hawking flux can be understood as follows. Contrary to the setup studied in [14] where the  $u$  and  $v$  sectors were completely decoupled in the dispersionless limit, there is no such decoupling in the present settings. The creation of left-moving quanta and the elastic scattering of  $u$  quanta into  $v$  quanta will thus be large, even when the dispersion plays no role. The above results thus suggest that for  $q$  close to 0.5, the  $u$ - $v$  mixing is small, and it gets large for extreme values of  $q$  near 0 and 1. To confirm this, we now turn to the properties of the flux of left-moving quanta,  $\bar{n}_\omega^v$ .

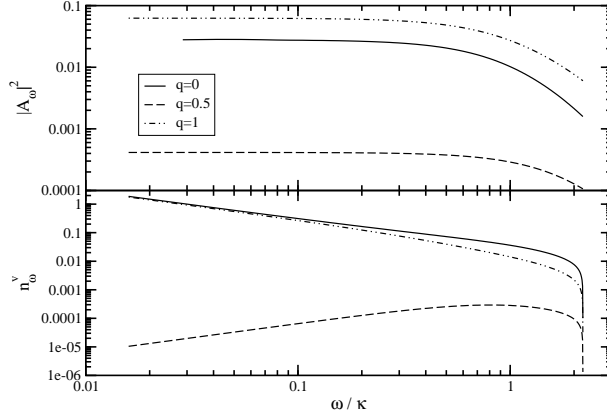


Figure 10:  $|A_\omega|^2$  (upper panel)

and  $n_\omega^v$  (lower panel) relative to those of Fig. 9.

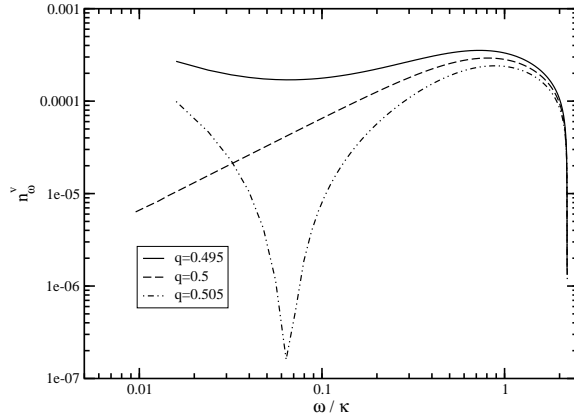


Figure 11:  $n_\omega^v$  versus  $\omega/\kappa$  for values of  $q$  near 0.5, namely 0.495, 0.5 and 0.505.  $D$  is fixed to 0.4 and  $\lambda = 17.15$ .

### 5. *Mixing of $u$ and $v$ quanta*

Figure 10 shows the particle flux of  $v$  quanta  $\bar{n}_\omega^v$  and the elastic scattering coefficient  $|A_\omega|^2$  as a function of  $\omega/\kappa$  for the same parameters as in Fig. 9.

At low frequencies,  $|A_\omega|^2$  is nearly constant. It is two orders of magnitude smaller for  $q = 0.5$  than for the other two values. It should be also noticed that  $|A_\omega|^2$  does not vanish for  $\omega \rightarrow \omega_{\max}$ , since both  $\phi_\omega^u$  and  $\phi_\omega^v$  remain well-defined above  $\omega_{\max}$  so that  $|A_\omega|^2$  connects smoothly to  $|R_\omega|^2$  at  $\omega = \omega_{\max}$ ).

Near  $\omega_{\max}$ ,  $\bar{n}_\omega^v$  goes to zero in the three cases. Instead, the low frequency behavior of  $\bar{n}_\omega^v$  changes dramatically depending on the value of  $q$ . First, the curves corresponding to  $q = 0$  and  $q = 1$  join at low frequencies, and are proportional there to  $1/\omega$ . This behavior in  $1/\omega$

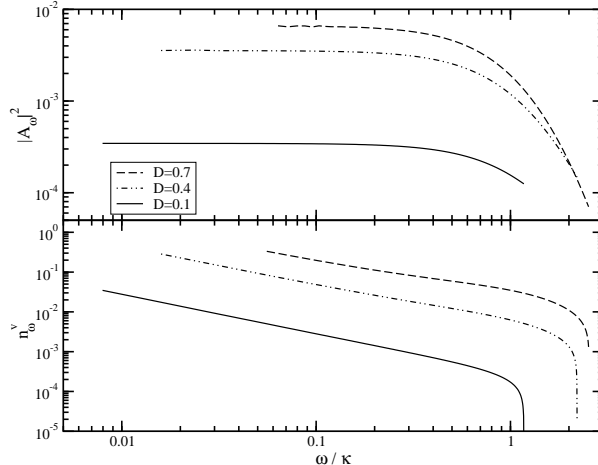


Figure 12:  $|A_\omega|^2$  (upper plot) and  $\bar{n}_\omega^v$  versus  $\omega/\kappa$ , for various values of  $D$ . The legend applies to both plots. The values of  $\lambda$  are identical to those of Fig. 6 and  $q$  is fixed to 0.3.

means that the energy flux  $\hbar\omega \bar{n}_\omega^v$  carried by the  $v$  quanta is constant and nonvanishing at low frequencies. Secondly, for  $q = 0.5$ ,  $\bar{n}_\omega^v$  stays everywhere below  $10^{-3}$  and is proportional to  $\omega$  at low frequencies. This proportionality with  $\omega$  was also obtained in the different setup of Ref. [14], and seems to indicate that the case  $q = 0.5$  (and not  $q = 1$  as one would have thought naively) is effectively similar to the setup of that reference.

To understand more precisely what happens in  $q = 0.5$ , we have represented in Fig. 11  $\bar{n}_\omega^v$  for  $D = 0.4$ ,  $\lambda = 17.15$ , and values of  $q$  close to 0.5. As  $q$  nears 0.5 from below,  $\bar{n}_\omega^v$  develops more structure and has a minimum. At low frequencies, it recovers the  $1/\omega$  behavior. For  $q$  above 0.5, the same structure is visible, but the minimum is much deeper. The curve still displays the  $1/\omega$  growth as  $\omega \rightarrow 0$ . Since it is difficult to reach very low values of  $\omega$ , we cannot state without doubt that  $q = 0.5$  does not have this behaviour. But it seems that it does not, and that  $\bar{n}_\omega^v$  continues decreasing as  $\omega$  when  $\omega \rightarrow 0$ . The existence of this particular point is most probably an artefact of our parameterization, Eq. (35), where  $v$  and  $c$  follow the same function. Nevertheless, these results have important experimental consequences: the qualitative conclusion that the  $u$ - $v$  mixing is lower when the horizon is formed by a combined variation of  $v$  and  $c$  rather than with a variation of  $c$  alone or  $v$  alone should not depend on the parameterization and should thus hold experimentally. If one wishes to obtain a thermal spectrum of  $u$  quanta outside the horizon, one should thus have both  $c$  and  $v$  vary.

In Fig. 12 the influence of  $D$  on the  $u$ - $v$  mixing coefficients  $\bar{n}_\omega^v$  and  $|A_\omega|^2$ , for  $q = 0.3$ . Both

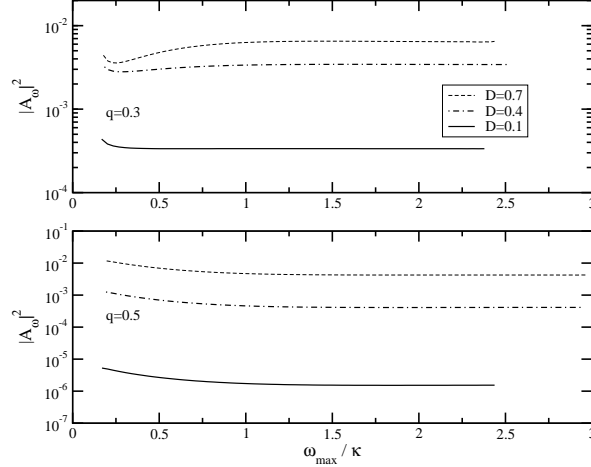


Figure 13:  $|A_\omega|^2$  evaluated for  $\hbar\omega = k_B T_H$ , versus  $\omega_{\max}/\kappa$  for  $D = 0.1$ ,  $D = 0.4$  and  $D = 0.7$ .  $q$  is fixed to 0.3 in the upper plot and 0.5 in the lower one.

the creation of  $v$  quanta and the elastic scattering coefficient  $A_\omega$  are significantly affected by  $D$  and increase by more than one order of magnitude between  $D = 0.1$  and  $D = 0.7$ . This will have important consequences when taking into account an initial temperature.

### 6. Dispersionless elastic scattering

It is instructive to look at the behavior of  $|A_{\omega_H}|^2$  evaluated for  $\hbar\omega_H = k_B T_H$  as a function of  $\omega_{\max}/\kappa$ , and for fixed values of  $D$  and  $q$ . It is shown in Fig. 13. When  $\omega_{\max}/\kappa$  is greater than about 2,  $|A_{\omega_H}|^2$  becomes nearly constant, with a value that depends on  $D$  and  $q$ . This means that for large  $\omega_{\max}/\kappa$ , the dispersion no longer plays any role. This is to be opposed to what was found in [14], where  $|A_{\omega_H}|^2$  scaled approximately as  $\lambda^{-4}$ . The reason is that in a BEC, the wave equation Eq. (17) does not factorize into a  $u$  and a  $v$  part in the dispersionless limit  $\lambda \rightarrow \infty$ . Thus, there is always some elastic scattering between  $u$  and  $v$  modes. What Fig. 13 shows is that the dispersionless value of  $|A_{\omega_H}|^2$  is quickly reached, or equivalently that the  $\lambda$ -dependent contributions vanish rapidly for increasing  $\lambda$ . This  $\lambda$ -independent elastic scattering exists also for  $q = 0.5$ , whereas we have seen that in this case  $\bar{n}_\omega^v$  has a behavior similar to the corresponding one in [14]. This is somewhat surprising.

Note finally that, since  $|A_\omega|^2$  is nearly constant in  $\omega$ , see Fig. 10 and Fig. 12, the value  $|A_{\omega_H}|^2$  for some  $(D, q)$  in the regime where  $\lambda$  plays no role actually gives  $|A_\omega|^2$  for all  $\omega$ .

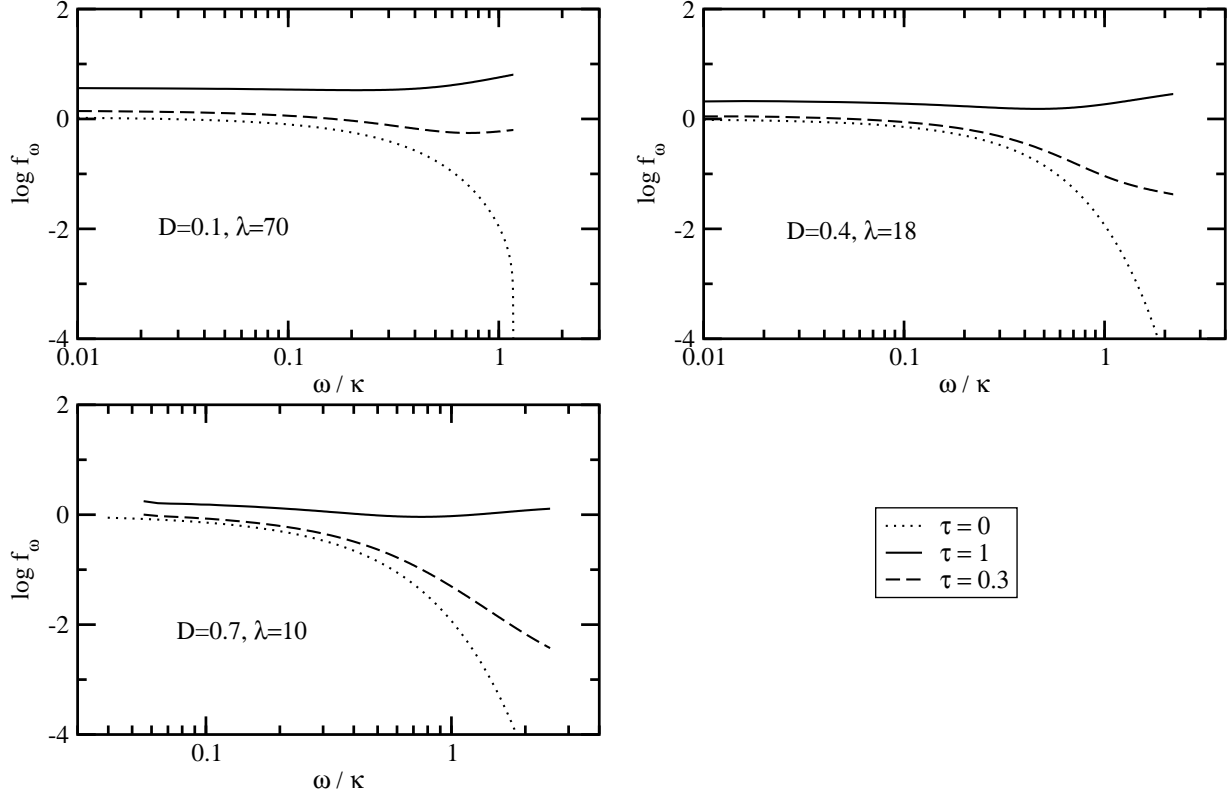


Figure 14: Energy flux emitted to the right of the horizon.  $q$  is fixed to 0.3. The dotted spectra are those of Fig. 6. The values  $\tau = 1$  (solid lines) and  $\tau = 0.3$  (dashed lines) correspond respectively to an initial temperature  $T_{\text{res}} = 30$  nK and  $T_{\text{res}} = 10$  nK, see Eq. (92).

### C. Spectral properties with an initial temperature

As pointed out in Secs. III E 2 and IV A, the residual temperature of a condensate is expected to be about two orders of magnitude higher than  $T_H$ . The spectra of the previous sections are thus unlikely to be found, and it is necessary to include the effects due to an initial temperature. This is easily done using Eq. (59) and the numerical values of the coefficients of the Bogoliubov transformation. Assuming that the three initial occupation numbers are characterized by a common comoving temperature, they are given by Eq. (57). Their calculation reduces to the computation of the functions  $\Omega^{in}(\omega)$  for the three types of modes, which is easily done by solving Eq. (36). Since  $\Omega^{in,a}$  are three nontrivial functions of  $\omega$ , the initial distributions are not Planckian in  $\omega$ .

The energy spectrum emitted to the right of the horizon, with a nonzero initial temper-

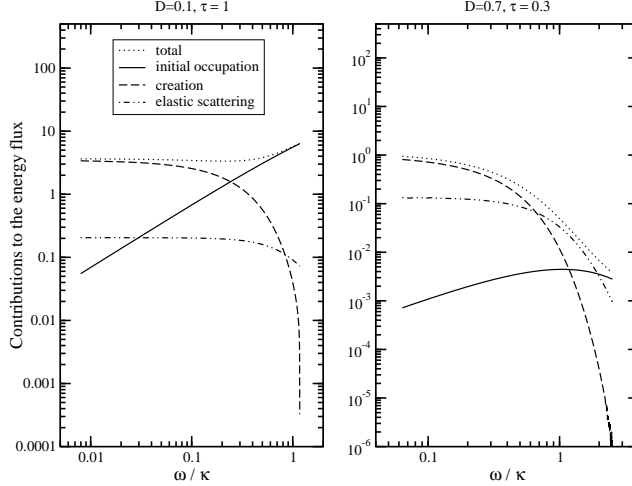


Figure 15: Different contributions to the energy flux to the right of the horizon. Left plot:  $D = 0.1$ ,  $\tau = 1$ . Right plot:  $D = 0.7$ ,  $\tau = 0.3$ .

ature, is defined as

$$f_{\omega}^{\text{fin}} = 2\pi \frac{\omega}{\kappa} n_{\omega}^{\text{fin}}. \quad (100)$$

It is represented in Fig. 14 for the same set of parameters as in Fig. 6. Two values of the initial temperature are considered: a conservative one,  $T_{\text{res}} = 30$  nK, and an optimistic one,  $T_{\text{res}} = 10$  nK. With the notations and the constraints of Sec. IV A, they correspond to  $\tau = 1$  and  $\tau = 0.3$  respectively. For  $D = 0.1$ ,  $D = 0.4$  and  $D = 0.7$  the ratio  $T_{\text{res}}/T_H$  is respectively 300, 75 and 43 when  $\tau = 1$ , and 90, 23 and 13, when  $\tau = 0.3$ .

The spectra differ greatly from those at zero temperature, and have a nontrivial behavior. Without surprise, they no longer vanish when approaching  $\omega_{\text{max}}$  because neither  $\bar{n}^{\text{in}}$  nor  $|A_{\omega}|^2$  do. The most interesting point is that for  $D = 0.4$  and  $0.7$  and the lower value of  $\tau$ , the spectra follow relatively closely the zero-temperature ones until  $\omega \simeq \kappa$ . Thus, for frequencies below  $\kappa$ , large values of  $D$ , and low initial temperatures, the measure of the phonon energy spectrum to the right gives a good estimate of the zero-temperature flux (i.e., Hawking radiation).

To better understand these spectra, we show in Fig. 15 the contributions to the energy flux of each of the three terms in Eq. (59), along with the full spectrum, in the two extreme cases  $D = 0.1$  with  $\tau = 1$ , and  $D = 0.7$  with  $\tau = 0.3$ .

In both cases, at high frequencies, the initial distribution  $\bar{n}_{\omega}^{\text{in}}$  largely dominates the spectrum, and all we see is just the flux of the initial quanta. At low frequencies instead, the main

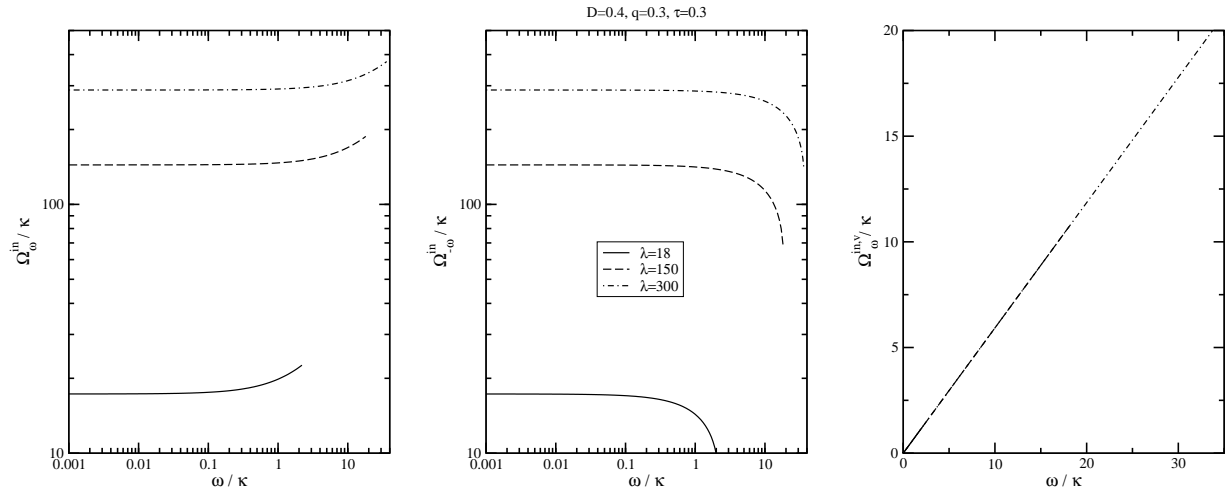


Figure 16: Initial proper frequency  $\Omega^{in}/\kappa$  as a function of  $\omega/\kappa$  for the  $u, \omega$  (left plot),  $u, -\omega$  (middle plot) and  $v, \omega$  modes (right plot), for  $D = 0.4$ ,  $q = 0.3$  and  $\tau = 0.3$ , and different values of  $\lambda$ . The legend applies to all plots.

contribution comes from the spontaneous plus stimulated emission term  $|\beta_{\omega}|^2(1 + \bar{n}_{\omega}^{in} + \bar{n}_{-\omega}^{in})$ , called “creation term” in Fig. 15. For  $D = 0.1$ , the  $u - v$  scattering term is small and never dominates, but it is never completely negligible. The contribution from  $|A_{\omega}|^2 \bar{n}_{\omega}^{in, v}$  quickly becomes comparable to the exponentially decreasing stimulated emission.

For  $D = 0.7$ , this contribution is not much smaller than the creation term at low frequencies, as could be expected from the results of Fig. 12. On the other hand, the contribution from  $\bar{n}_{\omega}^{in}$  long remains very small compared to the other two, until about  $\omega = \kappa$ . Thus the creation+stimulated emission term is actually dominated by the Hawking pair creation effect, since  $\bar{n}_{-\omega}^{in}$  is close to  $\bar{n}_{\omega}^{in}$ . This explains the relative similarity between the spectra with  $\tau = 0.3$  and  $\tau = 1$  in Fig. 14, when  $D = 0.7$ .

In brief, the main lesson from these plots is that, in general, there is no clear hierarchy between the various contributions in  $\bar{n}_{\omega}^{fin}$ , something which makes the interpretation of a measurement highly nontrivial. Nevertheless, let us try to identify what the optimal conditions are for such a detection.

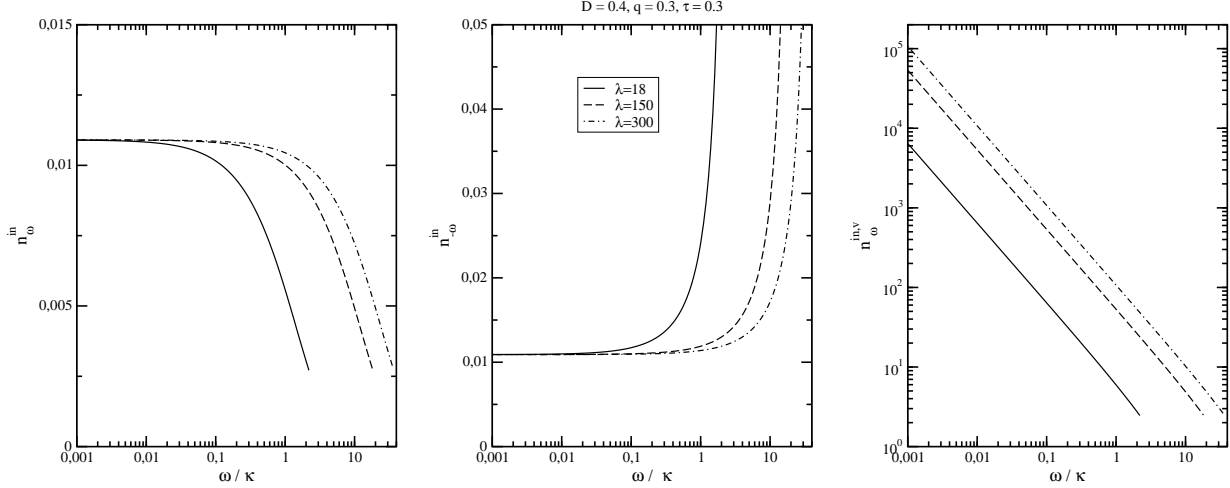


Figure 17: Initial occupation numbers  $n_{\omega}^{in}$  (left plot),  $n_{-\omega}^{in}$  (middle plot) and  $n_{\omega}^{in,v}$  (right plot) versus  $\omega/\kappa$ , for the same values of the parameters as in Fig. 16.

### 1. Optimal experimental conditions

The comoving frequency  $\Omega$  of the right-moving quanta is strongly redshifted in the black hole geometry, which implies that the initial  $\Omega^{in}(\omega)$  is much larger than  $\omega$  for these quanta. Since the integrated redshift increases with  $\lambda$ , one could ask whether lowering the Hawking temperature with respect to the initial temperature  $T_{\text{res}}$ , with a fixed value of  $D$ , could not improve the results above. This could be easily achieved by letting the flow velocity and the sound speed vary on a distance greater than  $10\xi_0$ . Then one would have  $\lambda \propto \frac{1}{D}$  like in Eq. (88), but with a larger proportionality factor. If the increase of the redshift were such that  $\Omega^{in}/T_{\text{res}}$  would increase with  $\lambda$ , the initial occupation numbers  $n_{\omega}^{in}$  and  $n_{-\omega}^{in}$  would decrease exponentially, and one could hope to have the stimulated plus creation term dominate over the other two on a larger interval of frequency  $\omega$ . This is not the case however, as we now explain.

The initial proper frequency  $\Omega^{in}(\omega)/\kappa$  for the three types of modes is shown in Fig. 16, for  $D = 0.4$ ,  $q = 0.3$ , and different values of  $\lambda$ . As expected, at a given  $\omega$ ,  $\Omega^{in,u}/\kappa$  is an increasing function of  $\lambda$ . However it scales only as  $\lambda$ , and since the ratio  $T_{\text{res}}/T_H$  also is proportional to  $\lambda$ ,  $\Omega^{in,u}/T_{\text{res}}$  hardly changes with  $\lambda$ . On the other hand, the left movers suffer almost no redshift, and  $\Omega^{in,v}$  has almost no dependence on  $\lambda$ . Thus when  $\lambda$  increases,  $\Omega^{in,v}/T_{\text{res}}$  decreases as  $1/\lambda$  and the initial occupation number of the  $v$  modes increases as  $\lambda$  for a given  $\omega$ .

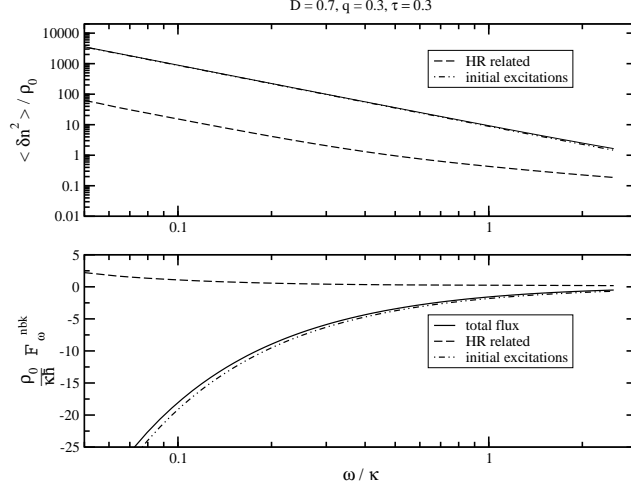


Figure 18: Density fluctuations divided by  $\rho_0$  (upper plot) and  $\rho_0 \mathcal{F}_\omega^{\text{nbk}} / \hbar \kappa$  (lower plot) as functions of  $\omega / \kappa$ , for  $D = 0.7$ ,  $q = 0.3$  and  $\tau = 0.3$ . “HR related” refers to the contribution weighted by  $n_\omega^{f, \text{in}} + 1/2$  and “initial excitations” to the one weighted by  $n_\omega^{v, \text{in}} + 1/2$ . The total density fluctuations are not explicitly shown because they are undistinguishable from the contribution of the initial excitations.

These remarks are summarized in Fig. 17, where the occupation numbers  $\bar{n}_\omega^{in}$  of Eq. (57) are represented for the same parameters as in Fig. 16.  $\bar{n}_\omega^{in}$  and  $\bar{n}_{-\omega}^{in}$  are almost equal and, more importantly, do not change with  $\lambda$  at low frequencies.  $\bar{n}_\omega^{in, v}$  on the other hand explodes when  $\lambda$  increases. Since  $|A_\omega|^2$  does not depend on  $\lambda$  in first approximation, the consequence is that the scattering contribution in  $\bar{n}_\omega^{f, \text{in}}$  dominates at low frequencies when  $\lambda$  increases, since the other contributions remain unchanged. In conclusion, there is no gain in lowering  $T_H$ .

In fact, as can be seen from the figures of the previous section, the optimal conditions to be able to measure directly the zero temperature flux  $f_\omega$  are found when there is a large relative variation of  $c + v$  on the smallest possible distance, that is the largest possible  $D$  with the smallest possible  $\lambda$ . Remember also that  $c$  and  $v$  should contribute nearly equally to the variation, for  $|A_\omega|^2$  to be as small as possible.

## 2. Density fluctuations and atom flux

As explained in Sec. III E 3, the flux  $f_\omega$  studied in the previous sections is observable only if one can distinguish experimentally between left- and right-moving phonons. It is

thus important to address the question whether the easily accessible density fluctuations also contain some signature of the particle creation process. The function  $\rho_0 G_\omega^{in}$  of Eq. (64), evaluated in the coincidence point limit in the right asymptotic region, is represented in the upper plot of Fig. 18 for  $D = 0.7$ ,  $q = 0.3$  and  $\tau = 0.3$ . This quantity is independent of  $\rho_0$  and is proportional to the density fluctuations  $\langle \delta n_\omega^2 \rangle / \rho_0^2$ , up to a factor  $\rho_0$  (which is constant in the right asymptotic region). In the lower plot,  $\mathcal{F}_\omega^{\text{nbk}}$ , obtained by subtracting the background contributions proportional to  $k_0$  from  $\mathcal{F}_\omega$  defined in Eq. (68) (“nbk” stands for “nonbackground”) is represented, for the same set of parameters. In both cases, the contributions proportional respectively to  $n_\omega^{\text{fin}} + 1/2$  (referred to as “HR related” in the figure) and to  $n_\omega^{\text{in},v} + 1/2$  have been plotted separately. In the case of the density fluctuations, the former contribution is always at least one order of magnitude below the latter. For  $\omega < \kappa$ , that is, in the region where  $n_\omega^{\text{fin}}$  is mainly due to Hawking radiation, see Fig. 14, it is even two orders of magnitude smaller. This confirms the remark made in the theoretical analysis that no clear signature of Hawking radiation can be observed in the density fluctuations. The same is true for the atom flux. However, as pointed out in Sec. III G, one could hope to combine both observables to extract  $n_\omega^{\text{fin}}$ .

## V. CONCLUSIONS

In this work, we have presented a complete description of the scattering of the phonon modes propagating in stationary, one dimensional condensates that possess a sonic horizon. Our description is based on the BdG equation, and the scattering in the horizon region is expressed in terms of  $3 \times 3$  Bogoliubov transformations relating asymptotic one phonon modes. To our knowledge, this was never done before.

We have shown that this scattering affects two types of observables, local ones such as the density fluctuations, and the long distance density-density correlations. The former are governed by standard expectation values which are diagonal in the occupation number, see Eq. (64). On the contrary, the latter are determined by interference terms, Eq. (74), which involve states with different occupation numbers, and which reveal the entangled nature of the final state.

When taking into account the condensate temperature, the local observables are in general dominated by the initial distributions. Thus, they are not suited for revealing the existence

of the Hawking effect. Instead, the nonlocal density-density correlations are amplified by these initial distributions without having their correlation pattern modified (when the initial state is uncorrelated). Therefore they constitute the clearest indication that the Hawking effect is taking place.

In the last part, we have numerically integrated the BdG equation, and obtained the occupation numbers of the three kinds of phonons, both with and without an initial temperature. The main results are the following. Firstly, in the initial vacuum and when the  $u$ - $v$  mixing is small ( $q \simeq 0.5$ ), the spectrum of the outgoing (right-moving) phonons is Planckian, with a temperature determined by the gradient  $\kappa$  of Eq. (33), as soon as  $\omega_{\max}/\kappa \gtrsim 2$  and for frequencies  $\omega < \omega_{\max}$ , see Fig. 6. This result, derived directly from the BdG equation (without any further approximation), makes precise the domain of validity of the analogy between relativistic fields in black hole metrics and a phonon field in the corresponding “dumb hole”. When the  $u$ - $v$  mixing is not negligible, the spectrum deviates from the Planck spectrum, see Figs. 9, 10 and 11. This is due to grey body factors (that can also be computed to a good approximation using the gravitational analogy [38]).

Secondly, as for the detection of the analog HR in a BEC, if one can distinguish left- from right-moving phonons, the Hawking flux could be observable when the relative variation of  $c + v$  is large and happens on a small number of healing lengths. Instead, if they cannot be distinguished, local observables are completely dominated by the initial temperature of the condensate. One must then resort to nonlocal observables such as the long distance density-density correlations, that exhibit a clear pattern associated with particle creation from the horizon [11]. This pattern is not erased by an initial temperature. Instead, in this case, the correlations are amplified.

Thirdly, in Appendix B, we have established the relationship between the fluxes emitted by white and black hole flows. Even if it turns out that white hole flows can be stable, a detection of the Hawking effect would be more difficult because the initial phonons would be blue shifted and will thus dominate the expectation values of local observables.

## Acknowledgments

R.P. is grateful to Roberto Balbinot for many stimulating discussions over the last years, as well as his comments on an early version of this paper. We both would like to thank the

participants of the workshop “Towards the observation of Hawking radiation in condensed matter systems” (<http://www.uv.es/workshopEHR/>) held at IFIC in Valencia in February 2009 for interesting remarks following our presentation.

## Appendix A: NONSTATIONARY CASE

### 1. 1D condensates

In this Appendix we consider nonstationary (one dimensional) condensates. As we shall see, little is modified when compared with the stationary case studied in the body of the paper.

In the mean field approximation, the condensate is now described by

$$\Psi_0(t, x) = \sqrt{\rho_0(x, t)} e^{iW_0(t, x)}. \quad (\text{A1})$$

This wave satisfies Eq. (5) where the external potential  $V$ , and the effective coupling  $g$  now depend both on  $x$  and  $t$ . (As pointed out in [11], some tuning of  $V$  and  $g$  might be necessary not to produce time dependent effects that might hide the Hawking radiation.) The conservation of the number of atoms follows from Eq. (5), and gives the continuity equation

$$\partial_t \rho_0 + \partial_x (\rho_0 v) = 0, \quad (\text{A2})$$

where  $v(t, x) = \hbar k_0(t, x)/m$  is the velocity of the condensate, and  $k_0(t, x) = \partial_x W_0(t, x)$  its wave vector. Plugging Eq. (A1) into Eq. (5) and using Eq. (A2) still gives Eq. (8) where  $\omega_0(t, x) = -\partial_t W_0$  is the lab frequency. (When considering nonstationary condensates, the notion of the preferred stationary Galilean frame disappears.)

Because of Eq. (A2), the condensate is still characterized by  $v(t, x)$  and the speed of sound

$$c^2(t, x) = g(t, x) \frac{\rho_0(t, x)}{m}. \quad (\text{A3})$$

### 2. Bogoliubov-de Gennes equation

As in Sec. II, the field is decomposed into its condensate and fluctuation parts:  $\Psi = \Psi_0 + \tilde{\phi}$ . At the linearized level, the latter still obeys Eq. (10). As before it is convenient to work

with the relative fluctuation  $\phi$  defined in Eq. (11). Then, using Eqs. (A1, A3), one still gets Eq. (12), which can be rewritten in the present case as

$$i\hbar(\partial_t + v\partial_x)\phi = T_\rho\phi + mc^2[\phi + \phi^\dagger]. \quad (\text{A4})$$

To get the  $c$ -number modes which shall be used to proceed to the second quantization, we look for a complete family of doublets  $W_j = (\phi_j, \varphi_j)$ , where the index  $j$  now does not correspond to a conserved quantum number. This complete family enters  $\phi$  as in Eq. (13):

$$\phi(t, x) = \sum_j \hat{a}_j \phi_j(t, x) + \hat{a}_j^\dagger (\varphi_j(t, x))^*, \quad (\text{A5})$$

where  $\hat{a}_j$  and  $\hat{a}_j^\dagger$  are annihilation and destruction operators, with which one can construct the phonon Fock space. However, contrary to the case studied in the text, there is in general no clear interpretation of the vectors in this Fock space in terms of particle content, and the notion of phonons is inherently ambiguous. The notion of phonon can be recovered if the condensate is stationary in the asymptotic past and the asymptotic future. In that case, one can define two Fock spaces, the in one and the out one, whose states have definite particle content in the asymptotic past and future respectively, if only locally in space. This is very similar to but generalizes what is described in the text, where an unambiguous notion of (quasi) particle could only be defined thanks to the asymptotic flatness of the metric.

Inserting Eq. (A5) in Eq. (A4) and taking the commutator with  $\hat{a}_j$  and  $\hat{a}_j^\dagger$  yields:

$$\begin{aligned} [i\hbar(\partial_t + v\partial_x) - T_\rho - mc^2] \phi_j &= mc^2 \varphi_j, \\ [-i\hbar(\partial_t + v\partial_x) - T_\rho - mc^2] \varphi_j &= mc^2 \phi_j. \end{aligned} \quad (\text{A6})$$

As in the body of the paper, one can eliminate  $\varphi_j$  to obtain a single equation for  $\phi$ . Repeating the same steps one gets

$$\left\{ [\hbar(\partial_t + v\partial_x) - iT_\rho] \frac{1}{c^2} [\hbar(\partial_t + v\partial_x) + iT_\rho] + 2mT_\rho \right\} \phi_j = 0. \quad (\text{A7})$$

One verifies that  $\varphi_j^*$  obeys the same equation.

We notice that all kinetic terms are of the form of Eq. (15). This is related to the fact that  $T_\rho$  is self-adjoint when using the scalar product of Eq. (40).

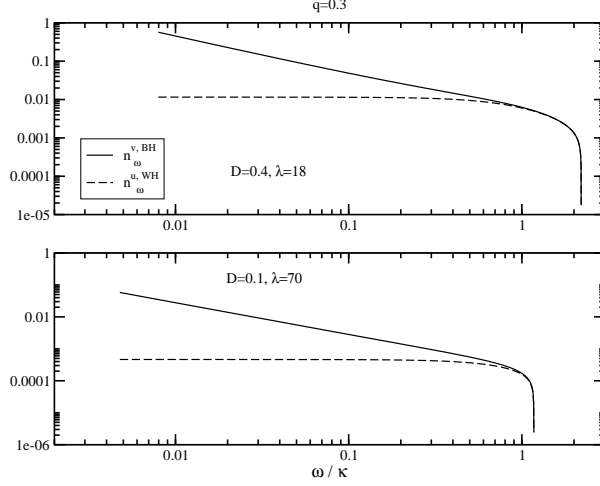


Figure 19: Occupation number of the  $v$  quanta for a BH ( $\bar{n}_\omega^v$ , solid line) and of the  $u$  quanta for the corresponding WH under the transformation (B1) ( $\bar{n}_\omega^{\text{WH},u}$ , dashed line), as functions of  $\omega/\kappa$  for  $q = 0.3$  and  $D = 0.4$  (upper plot) and  $D = 0.1$  (lower plot).

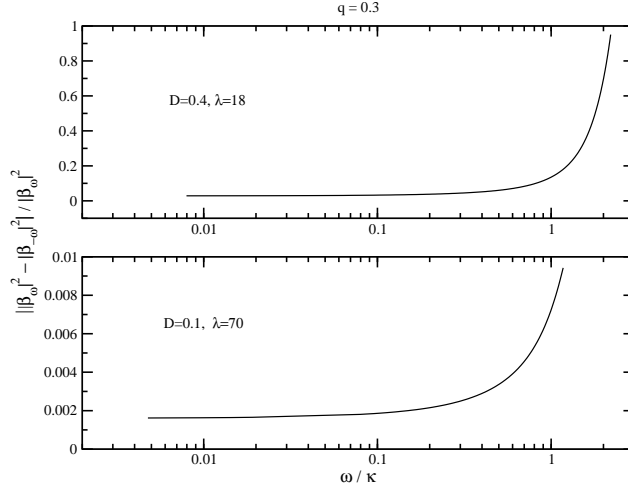


Figure 20: Relative difference  $||\beta_\omega|^2 - |\beta_{-\omega}|^2| / |\beta_\omega|^2$  as a function of  $\omega$ . Same parameters as in Fig. 19.

## Appendix B: WHITE HOLES

So far we only considered condensate flows that possess a sonic horizon which is analogous to that of a black hole. However sonic horizons which act as a white hole are closely related

to the black hole ones. Indeed, the transformation

$$\begin{aligned} v(x) &\rightarrow -v(x), \\ c(x) &\rightarrow c(x), \end{aligned} \tag{B1}$$

transforms the profile studied in the text, Eq. (34), into a white hole profile, in which the characteristics focus forward in time, see Eq. (32) with  $\kappa < 0$ . (This equation now applies to the left-moving modes, so that the quanta mainly produced are left-moving ones.)

The equivalent of Eq. (A7) in this WH profile reads:

$$\left\{ [\hbar(\partial_t - v\partial_x) - iT_\rho] \frac{1}{c^2} [\hbar(\partial_t - v\partial_x) + iT_\rho] + 2mT_\rho \right\} \phi_j = 0. \tag{B2}$$

Under a time-reversal  $t \rightarrow -t$ , Eq. (B2) becomes the complex conjugate of Eq. (A7). This proves that there is a one-to-one mapping given by:

$$\mathcal{T} : \phi_j^{\text{BH}}(t, x) \mapsto \phi_j^{\text{WH}}(t, x) = [\phi_j^{\text{BH}}(-t, x)]^*. \tag{B3}$$

The same relation holds between  $\varphi_j^{\text{BH}}$  et  $\varphi_j^{\text{WH}}$ . The doublets  $W_j^{\text{WH}}$  and  $W_j^{\text{BH}}$  related by Eq. (B3) thus have the same norm for the scalar product (40).

With these remarks, it is manifest that in a stationary WH flow, when working at fixed frequency  $\omega$ , the modes:

$$\begin{aligned} \phi_\omega^{v,in,\text{WH}}(t, x) &= e^{-i\omega t} [\phi_\omega^{u,out,\text{BH}}(x)]^*, \\ \phi_{-\omega}^{v,in,\text{WH}}(t, x) &= e^{-i\omega t} [\phi_{-\omega}^{u,out,\text{BH}}(x)]^*, \\ \phi_\omega^{u,in,\text{WH}}(t, x) &= e^{-i\omega t} [\phi_\omega^{v,out,\text{BH}}(x)]^*, \end{aligned} \tag{B4}$$

(and similarly for  $\varphi_\omega^{i,in,\text{WH}}$ ) form a complete in basis. Notice that the in/out character and the  $u/v$  character of the modes is interchanged between the BH and the WH. Indeed, because of the time-reversal symmetry, the phase and group velocities of the modes change sign. The Bogoliubov transformation relating the in to the out WH modes is thus the inverse of (53). This implies that when dealing with a WH flow in the initial vacuum, instead of Eq. (56), the mean occupation numbers of emitted quanta are

$$\begin{aligned} \bar{n}_\omega^{\text{WH}} &= |\beta_{-\omega}|^2, \\ \bar{n}_\omega^{u,\text{WH}} &= |B_\omega|^2, \\ \bar{n}_{-\omega}^{\text{WH}} &= \bar{n}_\omega^{\text{WH}} + \bar{n}_\omega^{\text{WH},u} = \bar{n}_{-\omega}^{\text{BH}}. \end{aligned} \tag{B5}$$

The third line shows that the total number of produced pairs is equal to that for the corresponding BH. However since  $|\beta_\omega|^2 \neq |\beta_{-\omega}|^2$ , the repartition of the quanta with positive  $\omega$  into left and right movers differs.

Before considering the implication of these relations, it is worth noting that only one quantity governs all differences between the occupation numbers and the elastic scattering in the WH and BH cases. Indeed, Eq. (B5) (or the third equation in (56)) shows that

$$|\beta_\omega|^2 + |\tilde{B}_\omega|^2 = |\beta_{-\omega}|^2 + |B_\omega|^2, \quad (\text{B6})$$

while the conservation of the norm of  $\phi_\omega^{u,\text{out},\text{BH}}$  and of  $\phi_\omega^{u,\text{in},\text{BH}}$  gives:

$$|\alpha_\omega|^2 + |\tilde{A}_\omega|^2 - |\beta_{-\omega}|^2 = |\alpha_\omega|^2 + |A_\omega|^2 - |\beta_\omega|^2 (= 1). \quad (\text{B7})$$

Thus,

$$|\beta_\omega|^2 - |\beta_{-\omega}|^2 = |B_\omega|^2 - |\tilde{B}_\omega|^2 = |A_\omega|^2 - |\tilde{A}_\omega|^2. \quad (\text{B8})$$

The relative difference between the occupation numbers in the BH and WH cases is small whenever the  $u$ - $v$  mixing coefficients are small, see for instance Sec. V C 3 in [14]. In the case of a BEC, however, the  $u$ - $v$  mixing coefficients are not necessarily small and can even grow as  $1/\omega$  at low frequencies, see Sec. IV B 5.

To further analyze the difference between WH and BH fluxes, in Fig. 19, we have represented  $|B_\omega|^2$  and  $|\tilde{B}_\omega|^2$  for  $q = 0.3$  and two values of  $(D, \lambda)$ . Contrary to  $|\tilde{B}_\omega|^2$  that grows as  $1/\omega$ ,  $|B_\omega|^2$  is nearly constant at low frequencies, so that their difference grows like  $1/\omega$ . The consequence of this is that the relative difference  $(|\beta_\omega|^2 - |\beta_{-\omega}|^2)/|\beta_\omega|^2$  tends to a constant at low frequencies, as is verified in Fig. 20, where this difference is shown for the same parameters as the previous figure. This constant value can be significant. For  $D = 0.4$  it is slightly greater than 1%; for  $D = 0.1$ , it is very small, of the order of 0.1%. For both values of  $D$ , the relative difference becomes important near  $\omega_{\text{max}}$ , but both  $|\beta_\omega|^2$  and  $|\beta_{-\omega}|^2$  vanish when reaching this frequency.

From Eq. (B5) several important lessons can be drawn. Firstly, we have established that, when starting with the vacuum state, the fluxes of phonons emitted by a WH flow are directly related to those of the corresponding BH flow.

Secondly, from this correspondance, the WH flows appear to be as stable as the corresponding BH flows. It should be stressed however that this conclusion is reached when using real frequencies  $\omega$ , and not taking into account the modes that are not asymptotically

bounded. Whether this implies that WH flows are stable is a moot point which deserves further study, see [39].

Thirdly, when expressed in the asymptotic regions in terms of the comoving frequency  $\Omega^a(\omega)$  (or the wave number  $k^a(\omega)$ ) the spectral properties of the WH fluxes are radically different from those of the corresponding BH. This is because, when considering a WH flow, the relationships between the comoving  $\Omega^a$  and the conserved frequency  $\omega$  are time reversed with respect to those for a BH. Hence, unlike what was found for a BH flow, Eq. (58) now determines the final values of the  $\Omega^a$  which are thus blueshifted. In the ideal case of an initial vacuum, this would be a great advantage. But when taking into account the nonvanishing temperature of the condensate, the initial occupation numbers are now given by  $n^{a,\text{in},\text{WH}}(\omega) = \left( e^{\Omega^{a,\text{out},\text{BH}}(\omega)/T_{\text{in}}} - 1 \right)^{-1}$ . Since  $\Omega^{a,\text{out},\text{BH}} \simeq \omega$ , and since  $T_{\text{in}} > T_H$ , these initial occupation numbers will always be much larger than the number of quanta created. There is no damping of the  $n^{a,\text{in}}(\omega)$  at small  $\omega$  as it was the case in BH flows, see Fig. 17, and thus even if one can distinguish left- from right-moving quanta, the detection of the analog Hawking radiation will be more difficult than in the corresponding BH.

- 
- [1] W. G. Unruh, Phys. Rev. Lett. **46**, 1351 (1981).
  - [2] T. Jacobson, Phys. Rev. D **44**, 1731 (1991).
  - [3] W. G. Unruh, Phys. Rev. D **51**, 2827 (1995).
  - [4] R. Brout, S. Massar, R. Parentani, and P. Spindel, Phys. Rev. D **52**, 4559 (1995), hep-th/9506121.
  - [5] S. Corley and T. Jacobson, Phys. Rev. D **54**, 1568 (1996), hep-th/9601073.
  - [6] C. Barcelo, S. Liberati, and M. Visser, Living Rev. Rel. **8**, 12 (2005), gr-qc/0505065.
  - [7] L. J. Garay, J. R. Anglin, J. I. Cirac, and P. Zoller, Phys. Rev. Lett. **85**, 4643 (2000), gr-qc/0002015.
  - [8] U. Leonhardt, T. Kiss, and P. Ohberg, J. Opt. B **5**, S42 (2003).
  - [9] F. Dalfovo, S. Giorgini, L. P. Pitaevskii, and S. Stringari, Rev. Mod. Phys. **71**, 463 (1999).
  - [10] R. Balbinot, A. Fabbri, S. Fagnocchi, A. Recati, and I. Carusotto, Phys. Rev. A **78**, 021603(R) (2008), 0711.4520.
  - [11] I. Carusotto, S. Fagnocchi, A. Recati, R. Balbinot, and A. Fabbri, New J. Phys. **10**, 103001

- (2008), 0803.0507.
- [12] S. Wüster (2008), 0805.1358.
- [13] R. Balbinot, A. Fabbri, S. Fagnocchi, and R. Parentani, Riv. Nuovo Cim. **28**, 1 (2005), gr-qc/0601079.
- [14] J. Macher and R. Parentani (2009), 0903.2224.
- [15] P. Jain, S. Weinfurtner, M. Visser, and C. W. Gardiner, Phys. Rev. A **76**, 033616 (2007), 0705.2077.
- [16] S. Weinfurtner, P. Jain, M. Visser, and C. W. Gardiner, Class. Quant. Grav. **26**, 065012 (2009), 0801.2673.
- [17] R. M. Wald, *Quantum field theory in curved space-time and black hole thermodynamics* (Chicago University Press, 1994).
- [18] J. M. Bardeen, B. Carter, and S. W. Hawking, Commun. Math. Phys. **31**, 161 (1973).
- [19] S. W. Hawking, Commun. Math. Phys. **43**, 199 (1975).
- [20] R. Brout, S. Massar, R. Parentani, and P. Spindel, Phys. Rept. **260**, 329 (1995), arXiv:0710.4345 [gr-qc].
- [21] S. A. Fulling, *Aspects of Quantum Field Theory in Curved Space-Time* (Cambridge University Press, 1989).
- [22] N. D. Birrell and P. C. W. Davies, *Quantum Fields in Curved Space* (Cambridge University Press, 1984).
- [23] S. Corley and T. Jacobson, Phys. Rev. D **59**, 124011 (1999), hep-th/9806203.
- [24] U. Leonhardt and T. G. Philbin, *in Quantum Analogues: From Phase Transitions to Black Holes and Cosmology* (Springer, Berlin, 2007), 0803.0669.
- [25] S. Massar and R. Parentani, Phys. Rev. D **54**, 7444 (1996).
- [26] R. D. Carlitz and R. S. Willey, Phys. Rev. D **36**, 2327 (1987).
- [27] R. D. Carlitz and R. S. Willey, Phys. Rev. D **36**, 2336 (1987).
- [28] R. M. Wald, Phys. Rev. D **13**, 3176 (1976).
- [29] C. Barcelo, S. Liberati, and M. Visser, Int. J. Mod. Phys. D **12**, 1641 (2003), gr-qc/0305061.
- [30] P. O. Fedichev and U. R. Fischer, Phys. Rev. A **69**, 033602 (2004), cond-mat/0303063.
- [31] V. F. Mukhanov, H. A. Feldman, and R. H. Brandenberger, Phys. Rept. **215**, 203 (1992).
- [32] D. Campo and R. Parentani, Phys. Rev. D **70**, 105020 (2004), gr-qc/0312055.
- [33] T. Jacobson and R. Parentani, Phys. Rev. D **76**, 024006 (2007), hep-th/0703233.

- [34] D. Campo and R. Parentani, Phys. Rev. D **72**, 045015 (2005), astro-ph/0505379.
- [35] D. Campo and R. Parentani, Phys. Rev. D **78**, 065044 (2008), 0805.0548.
- [36] D. Campo and R. Parentani, Phys. Rev. D **78**, 065045 (2008), 0805.0424.
- [37] D. Campo and R. Parentani, Phys. Rev. D **67**, 103522 (2003), gr-qc/0301044.
- [38] P. R. Anderson, talk given at the workshop “Towards the observation of Hawking radiation in condensed matter systems” (2009), URL <http://www.uv.es/workshopEHR>.
- [39] C. Barcelo, A. Cano, L. J. Garay, and G. Jannes, Phys. Rev. D **74**, 024008 (2006), gr-qc/0603089.